Construction and characterization of a full-length cDNA infectious clone of emerging porcine Seneca Valley Virus

by

Fangfeng Yuan

B.A., Qingdao Agricultural University, 2014

A THESIS

submitted in partial fulfillment of the requirements for the degree

MASTER OF SCIENCE

Department of Diagnostic Medicine and Pathobiology
College of Veterinary Medicine

KANSAS STATE UNIVERSITY
Manhattan, Kansas

2017

Approved by:

Major Professor
Ying Fang

Abstract

Seneca Valley Virus (SVV) causes vesicular disease in pigs. Vesicular lesions on the snout and coronary band of hoof mostly resemble lesions caused by Foot-and-Mouth Disease Virus (FMDV), which may lead to the foreign animal disease investigation. In 2015, Brazil experienced major outbreaks of SVV; then in July, sporadic cases of SVV were reported in United States and became a concern in swine industry. A reverse-genetic system serves as a major tool to study pathogenesis of the virus. In our study, a full-length cDNA infectious clone, pKS15-01-Clone, was constructed from an emerging Seneca Valley Virus (SVV; strain KS15-01). To explore the potential use as a viral backbone for expressing marker genes, the enhanced green fluorescent protein (EGFP)-tagged reporter virus (vKS15-01-EGFP) was generated using reverse genetics. Compared to the parental virus, the pKS15-01-Clone derived virus (vKS15-01-Clone) replicated efficiently in vitro and in vivo, and induced similar levels of neutralizing antibody and cytokine responses in infected animals. In contrast, the vKS15-01-EGFP virus showed impaired growth ability and induced lower level of immune response in infected animals. Lesions on the dorsal snout and coronary bands were observed in all pigs infected by parental virus KS15-01, but not in pigs infected with vKS15-01-Clone or vKS15-01-EGFP viruses. These results demonstrated that the infectious clone and EGFP reporter virus will be important tools in further elucidating the SVV pathogenesis and development of control measures.

Table of Contents

List of Figures v

List of Tables vi

Acknowledgements vii

Chapter 1 - Literature Review 1

Seneca Valley Virus - The Disease 1

Molecular biological features of SVV 3

Life cycle of SVV 4

Structural features of SVV capsid proteins 6

Chapter 2 - Construction and characterization of a full-length cDNA infectious clone of newly emerging porcine Seneca Valley Virus 11

Introduction 11

Materials and Methods 13

Cells and viruses 13

Construction of full-length cDNA clones of SVV KS15-01 14

Recovery of recombinant viruses 15

Identification of recombinant viruses 16

Monoclonal antibody (mAb) production 16

Western blot analysis 17

Immunofluorescence assay 18

Virus growth kinetics and plaque forming assay 19

Animal study 19

Quantitative RT-PCR 20

Neutralizing antibody assay 20

SVV specific antibody response 21

Analysis of swine cytokine response 21

Statistical analysis 22

Results 22

Construction of an infectious clone of emerging Seneca Valley Virus isolate KS15-01 .22

In vitro recovery and characterization of recombinant virus derived from Seneca Valley Virus full-length cDNA clone pKS15-01-Clone 23
Seneca Valley Virus infectious clone as a vector for expressing EGFP 24
Clinical observations in nursery pigs infected with the parental and recombinant Seneca Valley Virus 25
In vivo growth properties of the parental and recombinant Seneca Valley Virus in pigs 26
In vivo stability of mutations or insertions introduced in Seneca Valley Virus 27
Innate and adaptive immunity following infection with parental and recombinant Seneca Valley Virus 29
Figures and Tables 31
Discussion 48
Chapter 3 – Future research on SVV 54
References 57
Publisher's Permission for Reproducing Published Materials 62

List of Figures

Figure 1-1. Schematic diagram of SVV genome and virion. 7
Figure 1-2. Summary of picornavirus life cycle. 8
Figure 1-3. Protomer structure of SVV-001. 9
Figure 1-4. Phylogenetic tree of SVV P1 sequences 10
Figure 2-1. Schematic diagram of the full-length SVV genome and construction of the full-length cDNA clones. 37
Figure 2-2. Differentiation of the parental virus from the cloned virus and EGFP-tagged virus in infected cells. 38
Figure 2-3. Detection of the viral protein and EGFP expression in parental and recombinant virus- infected cells. 39
Figure 2-4. In vitro growth characterization of the parental and recombinant viruses. 40
Figure 2-5. Clinical signs and surface lesions observed on infected pigs. 41
Figure 2-6. Comparison of viral load in pigs inoculated with the parental and recombinant viruses. 43
Figure 2-7. Analysis the stability of molecular marker or reporter gene in recombinant viruses infected pigs. 44
Figure 2-8. IFN-α response in serum samples from pigs inoculated with the parental and recombinant viruses. 46
Figure 2-9. Neutralizing antibody titers in serum samples from pigs inoculated with the parental and recombinant viruses. 46
Figure 2-10. SVV specific antibody response in serum samples from pigs inoculated with parental and recombinant viruses. 47

List of Tables

Table 1. Nucleotide differences between the genome of parental virus SVV KS15-01 and full length cDNA clone pKS15-01-Clone 31

Table 2. Surface lesions on snout and coronary band of SVV KS15-01- infected pigs 32

Table 3. Primers for constructing full-length cDNA clone and sequencing viral genome 33

Table 4. Daily clinical observation from dpi 0 to dpi 14 35

Table 5. Rectal temperature record from dpi 0 to dpi 14 36

Acknowledgements

I would first like to express my sincere thankfulness to my Major professor, Dr. Ying Fang, for accepting me into this competitive lab and allowing me precious opportunities to grow as a researcher here during the past two years. I was fully influenced and convinced by the highly experimental standards here. It's under her guidance that allow me stepping into the heaven of science and further moving forward. Now I feel much more comfortable to pursue my future career goals.

Secondly, I would like to thank my graduate committee members, Dr. Bob Rowland and Dr. M.M. Chengappa, for their support and suggestions for my project. My sincere gratitude also goes to Dr. Jianfa Bai, Dr. Jamie Henningson, Dr. Benjamin Hause for their favors.

I also would like to thank all of my research team members in the lab for their kindly teaching and patient explanation of my questions. It's my pleasure to work with them. This includes Dr. Yanhua Li, Dr. Zhenhai Chen, Rui Guo, Pengcheng Shang, Yin Wang and Russell Ransburgh.

I would like to thank my elder uncle, Shishan Yuan, for his persistent guidance and help since I was a little kid. My interest in research on animal diseases and sciences was inspired and motivated by his guidance.

Finally, I would like to thank my parents, Shiwen Yuan and Xiuqin Dang, for their teaching, understanding and encouraging me all the way along.

Chapter 1 - Literature Review

Seneca Valley Virus and Porcine Idiopathic Vesicular Disease

Seneca Valley Virus (SVV) was first isolated at Genetic THERAPY Inc. (Gaithersburg, MD, USA) in 2002. It was serendipitously discovered as a contaminant during the cultivation of PER.C6 cell, which is transformed fetal retinoblast cells and was also presumably introduced through bovine serum or porcine trypsin source (Hales et al., 2008; Reddy et al., 2007). SVV was reported to be a replication-competent oncolytic virus and has selective tropism for cancers with neuroendocrine features including small cell lung cancer (SCLC) and several pediatric solid tumors, like retinoblastoma, neuroblastoma, and medulloblastoma, but does not infect normal human cells (Reddy et al., 2007). Due to its potential antineoplastic activity, Clinical trials has been tried to develop SVV as an anti-cancer therapeutic by virtual company Neotropix.

Seneca Valley Virus has been identified as the pathogen that causes porcine idiopathic vesicular disease. In June of 2007, a group of Canadian market pigs arrived at the facility in Minnesota exhibited ruptured vesicles along the coronary band of the hoof and coalescing erosions on the snout (Pasma et al., 2008). Foot-and-mouth disease virus, swine vesicular disease virus, vesicular stomatitis virus and vesicular exanthema virus were tested negative by Plum Island Animal Disease Center. Further testing identified the presence of Seneca Valley Virus, porcine enterovirus and porcine circovirus in 15 pigs (Pasma et al., 2008). From 1988 to 2001, even though seven SVV isolates were recovered from pigs in different locations in US, the clinical symptoms were not reported in detail. The disease has been reported in United States, Australia, Canada, New Zealand and most recently in Brazil (Leme

et al., 2015; Singh et al., 2012; Vannucci et al., 2015; Zhang et al., 2015). China also reported the first case of SVV infected pig in 2015 (Wu et al., 2016). Since July 2015, sporadic cases associated with vesicular lesions and neonatal mortality in swine have been reported in multiple regions of US, such as North Carolina, Illinois, California, Iowa, Minnesota etc (Hales et al., 2008; Knowles and Hallenbeck, 2005; Pasma et al., 2008). Brazil reported its first case of SVV infection in early 2015 (Leme et al., 2015), and an increasing number of cases continues to be reported. SVV strain referred in our study was obtained from pig nasal swabs in June 2015 (Hause et al., 2015). And it was also reported that the 2015 US SVV strain were most closely related to the SVV sequence obtained from Brazil. However, all these sequences are from a common ancestor in Canada (figure 1-4). This disease is growing to be a big problem in swine industry in the affected countries and there is significant concern regarding its potential to impact Europe and other countries around the world.

The clinical signs include ruptured or intact vesicles on a pig's snout, mouth (Singh et al., 2012), as well as lesions on the feet around the coronary bands. The breeding females may show anorexia, lethargy, or are febrile. Some sows may have fevers up to 105 °F. There have been reports of unexplained lameness, diarrhea in piglets prior to the emergence of vesicles or erosions (Singh et al., 2012). The mortality rate in neonatal piglets may increase and there is no record of SVV causing diseases in human. Clinical signs observed in SVV infected pigs cannot be distinguished from other vesicular diseases, such as foot-and-mouth disease, swine vesicular disease, and vesicular stomatitis (Singh et al., 2012). Any outbreaks of vesicular disease should be diagnosed to rule out FMDV infection, which is highly contagious and devastating. Few tools are used for SVV detection, which includes reverse

transcription-polymerase chain reaction (RT-PCR), real-time PCR, virus neutralizing assay. A quick and convenient tool to identify the presence of SVV in suspect cases will be helpful. Serological surveys demonstrated the presence of antibodies capable of neutralizing SVV-001 in pigs, cattle and mice, but not in humans (Zhang et al., 2015). There have been attempts to infect pigs with SVV-001 and its related isolates, but failed to demonstrate any specific disease (Hales et al., 2008; Knowles et al., 2006; Pasma et al., 2008; Yang et al., 2012). Although no clear association of the virus with disease in pigs was established, pigs are believed as the natural host for SVV due to the fact that the virus has been isolated from pigs. But transmission pathways, pathogenesis and epidemiology of SVV are still yet to be determined.

Molecular biological features of SVV

The full genome sequence of SVV was completed in 2008. SVV is a small, non-enveloped RNA virus. It belongs to family *Picornaviridae*, which also contains foot-and-mouth disease virus (FMDV) and swine vesicular disease virus (SVDV) (Adams et al., 2015; Hales et al., 2008; Graves, 1973; Inoue et al., 1989). SVV is the single species classified in the genus *Seneca Valley Virus* and shares most similarity with the genus *Cardiovirus* when aligning the P1, 2C, 3C and 3D protein sequences, but diverges greatly in the 2B and 3A polypeptides (Hales et al., 2008).

Like other picornaviruses, a positive-sense, single-stranded RNA genome that serves as a template for RNA replication and translation. The whole genome organization of SVV follows the typical L-4-3-4 layout. It includes a single open reading frame (ORF), which encodes a large polyprotein flanked by a long 5’ UTR and a shorter 3’ UTR with a poly(A)

tail (Hales et al., 2008; Rueckert and Wimmer, 1984). VPg, a virus-encoded peptide, covalently binds to the RNA 5' terminus and serves as a primer for initiation of RNA synthesis. Internal Ribosome Entry Site (IRES) located in the 5' UTR allows cell ribosome binding and initiation of protein synthesis in a manner independent on cap. The IRES in SVV was reported to have structural and functional similarities to that from members of *flaviviridae*, suggesting possible recombination events may occur between these two genomes (Willcocks et al., 2011). The first synthesized large polyprotein will undergo a series of cleavage processing events, which is mediated by virus-encoded protease and produce 11 mature virus proteins and numerous partially processed cleavage products (Hales et al., 2008). N-terminal portion of the polypeptide is P1 or capsid protein, followed by P2, P3, which are non-structural proteins.

Life cycle of SVV

Figure 1-1 presents the SVV genome organization and structure and figure 1-2 is a summary of the general life cycle of picornaviruses. Replication of SVV is exclusively in cytoplasm. It is predicted that entry into cells is achieved by receptor mediated endocytosis. However, host receptor responsible for binding to SVV is still under investigation (Sangita Venkataraman, 2008). After internalization, the virus undergoes uncoating, and viral RNA genome is released into cytoplasm. Cellular ribosomes land on IRES of 5' end and starts RNA translation. The viral polyprotein is processed rapidly both during and after translation. The protein processing cascade can be initiated by several primary cleavage events carried out in *cis*, then a series of *trans* cleavages by 3C protease, which is a chymotrypsin-like protease (J. Lindsay Whitton, 2005). The primary processing event involves uncoupling of

P1-2A region from the rest of viral polyprotein by ribosomal skipping which prevents the formation of Gly-Pro peptide bond. Cleavage events between Leader protein and P1, 2BC and P3 are carried out by 3C protease, which recognizes Gln/Gly, Gln/Ser or Glu/Asn pairs (Hales et al., 2008). Compared to cardioviruses, the most difference lies in the size of the 2A, which is considerably smaller in SVV. For SVV capsid P1 protein, the gene order is VP4, VP2, VP3, VP1, as is shown in Figure 1-1. VP4/ VP2/VP3/VP1 cleavage occurs between K/D, Q/G, H/S respectively (Hales et al., 2008). The Presence of 71 residues upstream of VP2 suggests the intermediate product, VP0, which was the precursor of VP4 and VP2. Notably, VP0 has a myristoylation motif, which may allow post-translational modification and more functions of the protein (Hales et al., 2008).

Replication of picornavirus RNA takes place in a viral replication complex, which is dependent on the 3D encoded protein, RNA-Dependent-RNA-Polymerase. Due to low replication fidelity, 3D is error prone and has error frequencies as high as 1 in 10^3 to 10^4 nucleotides, resulting in rapid virus mutation within the host (Jing-Yi Lin, 2009). Synthesis of the uridylylated VPg is the first step for viral RNA synthesis. After virions are packaged, they are exported out of the cell.

Senecavirus non-structural proteins have great potential to shut off host cell transcription and translation, achieved by cleavage of the cellular protein eIF-4G, which is a key factor in cap-dependent translation. It might also have strategies to limit cellular immune response by inhibition of MHC class I expression. It was reported that picornaviruses can prevent cell apoptosis, thus facilitates the establishment of viral persistence (J. Lindsay et al., 2005).

Structural features of SVV capsid proteins

The viral capsid protein plays a vital role in receptor binding and thus determines viral tropism and pathogenesis. The capsid features in icosahedral symmetry containing a tightly packaged viral genome. It is composed of 60 copies, each of four surface proteins known as VP1, VP2, VP3, VP4. VP1 to VP3 are the building blocks of outer shell of the virion, and have major neutralizing antigenic sites (Sangita et al., 2008). The small VP4 protein resides inside of the virion and binds to the nucleic acids. Figure 1-3 presents the protomer structure of SVV-001. There are several surface exposed loops, which may involve cell tropism and have particular importance. As figure 1-3 presents, the BC loop (50-74aa) and GH loop (185-215aa) located in VP1, loop Ⅱ (CD loop, 94-109aa), and the "Puff" (EF loop, 172-200aa) located in VP2, also the "Knob" (residues 57-73aa) is in VP3 subunit (Sangita et al., 2008). The VP1 G–H loop in Foot-and-mouth disease virus (FMDV) is reported to be a major antigenic site (Lawrence and Pacheco et al., 2013).

Figure 1-1. Schematic diagram of SVV genome and virion.

The capsid consists of a densely-packed icosahedral arrangement of 60 protomers, each consisting of 4 polypeptides, VP1, VP2, VP3 and VP4. VP4 is located on the internal side of the capsid. Viral genomic RNA has a viral protein (VPg) at its 5' end instead of a methylated nucleotide cap structure. The 5' end contains an internal ribosome entry site probably of type IV. The P1 region encodes the structural polypeptides. The P2 and P3 regions encode the nonstructural proteins associated with replication.

Figure adapted from http://viralzone.expasy.org.

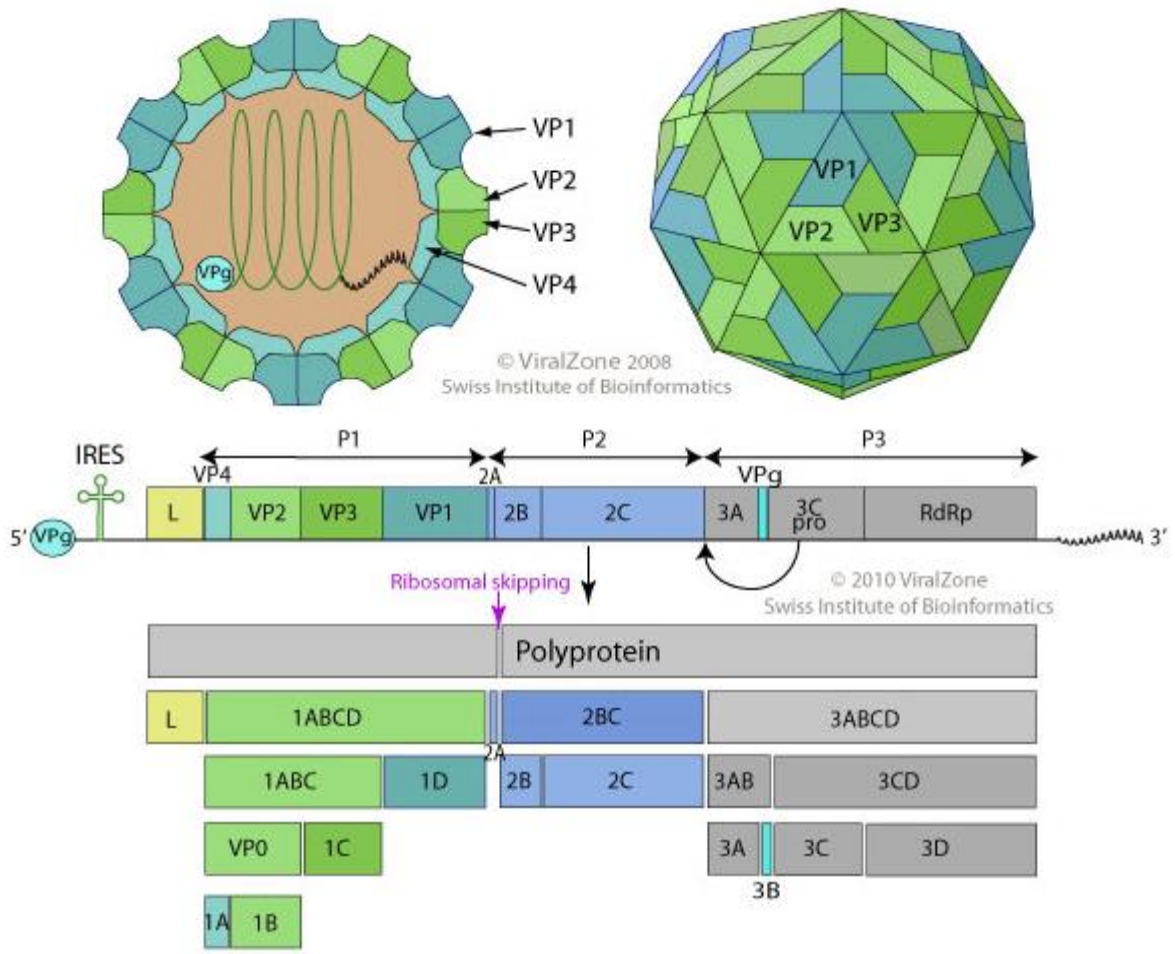

Figure 1-2. Summary of picornavirus life cycle.

(A). RNA with VPg at the 5' end is translated into one primary translation product (B) which is then cleaved (C). The positive strand genomic RNA also associates with an RNA polymerase that is bound to the cytoplasmic surface of vesicles, probably from the endoplasmic reticulum, and is copied to negative stand RNA. VPg is also at the 5' end of the negative strand (the poly U end) (D). The negative strand is copied to genomic positive strand RNA (E) which associates with the procapsid to form a 150S virus (G) that is released on cell lysis. Figure adapted from Margaret Hunt (2015).

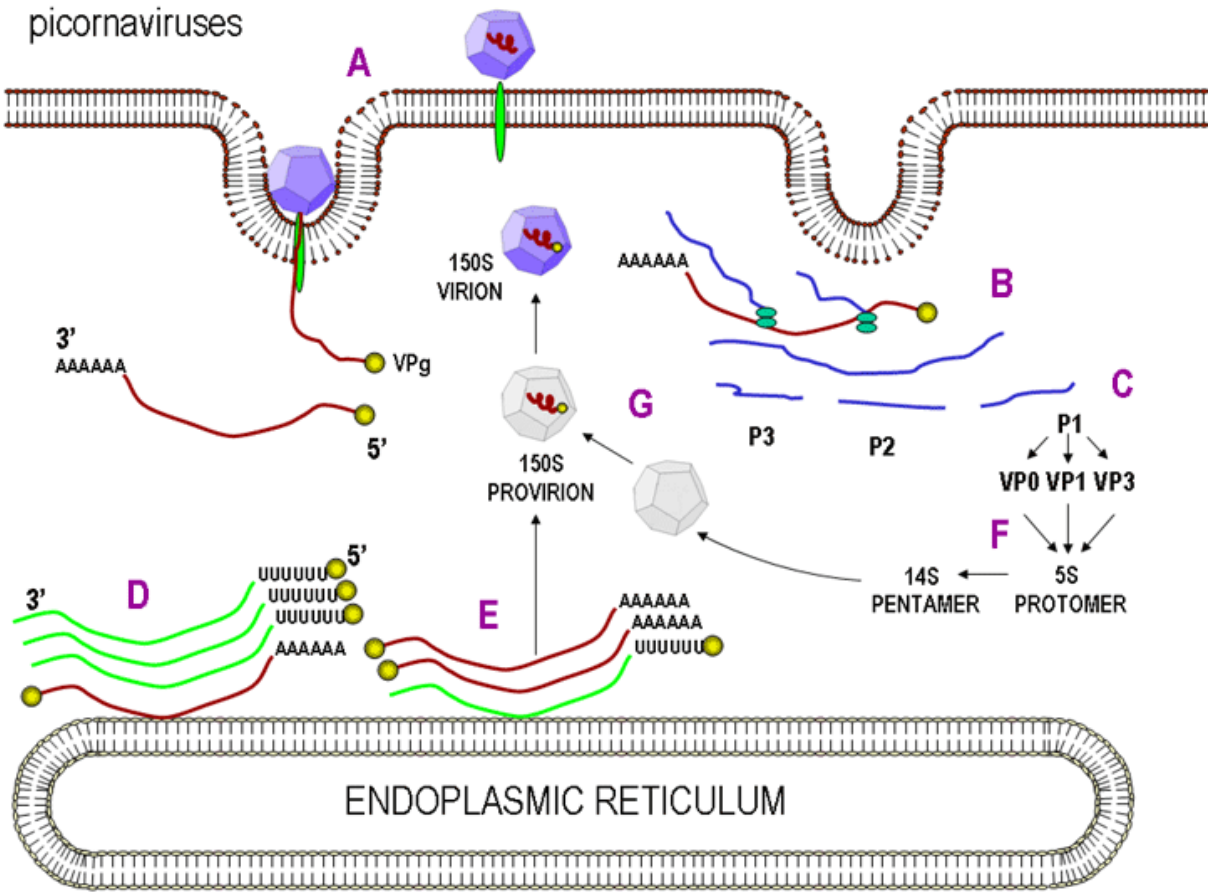

Figure 1-3. Protomer structure of SVV-001. Ribbon diagrams of SVV-001 protomer, (a) front view and (b) a side view, highlighting the different subunits and the prominent surface loops. VP1, VP2, VP3 and VP4 subunits are shown in blue, green, red and yellow respectively. Figure adapted from Sangita Venkataraman (2008).

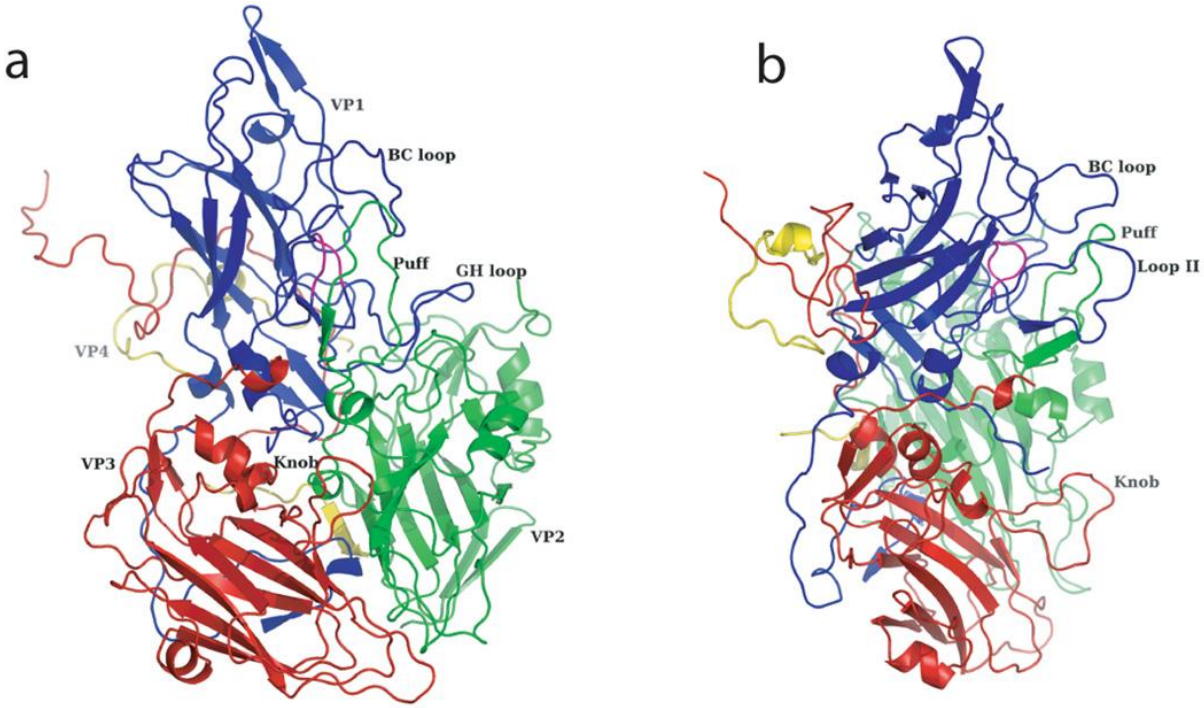

Figure 1-4. Phylogenetic tree of SVV P1 sequences.
Figure adapted from Ben M. Hause (2015).

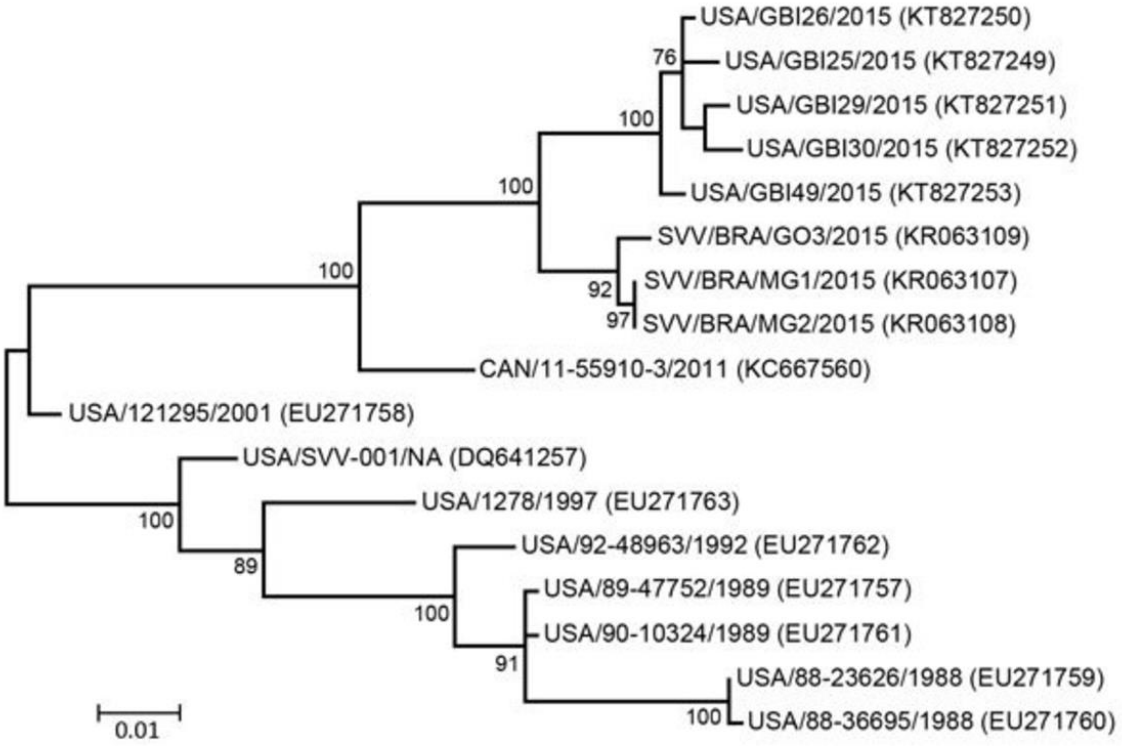

Chapter 2 - Construction and characterization of a full-length cDNA infectious clone of newly emerging porcine Seneca Valley Virus

Introduction

Seneca Valley Virus (SVV) is a single-stranded non-enveloped RNA virus. SVV belongs to the genus *Senecavirus,* family *Picornaviridae* (Adams et al., 2015; Hales et al., 2008). Important members in the family also include poliovirus, rhinovirus, hepatitis A virus, foot-and-mouth disease virus (FMDV) and swine vesicular disease virus (SVDV) (Graves, 1973; Inoue et al., 1989). The genome of SVV is a positive-sense RNA molecule ~7.3 kb in length. It contains a single open reading frame (ORF), encoding a large polyprotein, flanked by a long 5' untranslated region (UTR; ~ 668 nucleotides), and a short 3' UTR (~68 nucleotides) followed by a poly(A) tail. The viral polyprotein is predicted to be processed by virus-encoded proteases into 12 polypeptides in the standard picornavirus L-4-3-4 layout, with viral structural proteins encoded towards the 5' end of the genome, while non-structural proteins encoded at the 3' end (Hales et al., 2008; Rueckert and Wimmer, 1984). Primary cleavage events are predicted to involve a ribosome-skipping mechanism to separate P1–2A from 2BC–P3 (Donnelly et al., 2001) and a traditional proteolytic process by 3C protease to cleave between L and P1 and between 2BC and P3 (Hales et al., 2008). In comparison with other picornaviruses, sequence analysis of prototypic strain SVV-001 showed that the P1, 2C, 3C and 3D polypeptides regions were most closely related to those of cardioviruses, but other regions of the polyprotein differed considerably from those of the other known picornaviruses (Hales et al., 2008). Within its 5' UTR, the SVV RNA genome contains an internal ribosome entry site (IRES), which displays the secondary structural features that resemble the IRES

element (type IV IRES) of classical swine fever virus (CSFV) in the family *Flaviviridae*, suggesting recombination events might be occurred between the genomes of the *Picornaviridae* and *Flaviviridae* during persistent co-infection in pigs (Willcocks et al., 2011).

The first identification of SVV, known as SVV-001 isolate, was reported in 2002 from a PER.C6 cell culture. Thereafter, the virus was developed as an oncolytic agent due to its selective tropism for human tumor cells and also no observed pathogenicity in human and animals (Hales et al., 2008; Reddy et al., 2007). Subsequently, sporadic serologically similar SVV isolates have been identified from pig samples in the US and Canada (Hales et al., 2008; Knowles and Hallenbeck, 2005; Pasma et al., 2008). Phylogenetic analysis suggested those different isolates of SVV had a common ancestor (Knowles et al., 2006). Historically, the association of SVV with swine vesicular disease was speculative, since the virus had also been isolated from pigs without clinical symptoms, and experimentally inoculated pigs with SVV isolates were unable to reproduce the disease (Hales et al., 2008; Knowles et al., 2006; Pasma et al., 2008; Yang et al., 2012). Recently, case reports from Brazil, Canada, China and the US provided evidence that SVV is a potential causative agent of idiopathic vesicular disease in pigs (Leme et al., 2015; Singh et al., 2012; Vannucci et al., 2015; Wu et al., 2016; Zhang et al., 2015). In some of those pigs tested as SVV positive, clinical signs of anorexia, lethargy, lameness, and vesicular lesions were observed. Gross lesions could be found on the oral mucosa, snout, nares, distal limbs, especially around the coronary bands (Singh et al., 2012). These clinical presentations resemble those caused by other economically more devastating transboundary pathogens that caused vesicular disease, including vesicular

exanthema of swine virus (VESV), FMDV, and SVDV, which may lead to foreign animal disease investigations.

A reverse genetics system for SVV is needed to study the basic viral pathogenesis and develop modified live virus vaccines. Previously, a full-length cDNA infectious clone of SVV-001 was constructed (Poirier et al., 2012). However, it was developed as an anticancer agent, and the cloned viruses were not characterized for replication in pigs. In this study, we generated a full-length cDNA infectious clone of an emerging SVV, strain KS15-01. The *in vitro* and *in vivo* growth properties of the parental and cloned viruses were evaluated in cultured cells and nursery pigs. The availability of this infectious clone provides a powerful research tool for studying SVV pathogenic mechanisms and serves as a valuable backbone for future modified live virus vaccine development.

Materials and Methods

Cells and viruses

PK-15 and BHK-21 cells were cultured in Minimum Essential Medium (MEM) (Gibco, Carlsbad, CA) supplemented with 10% fetal bovine serum (Sigma-Aldrich, St. Louis, MO), antibiotics [100 units/ml of penicillin (Gibco, Carlsbad, CA) and 100 μg/ml of streptomycin (Gibco, Carlsbad, CA)] and 0.25 μg/ml fungizone (Gibco, Carlsbad, CA) at 37 °C and 5% CO_2. The wild-type SVV was obtained from a diagnostic case submitted to KSVDL in 2015. Initially, the nasal swab samples were analyzed by next generation sequencing and SVV genome sequence was detected (Hause et al., 2016). Subsequently, the virus was isolated from a SVV positive nasal swab sample and plaque purified, designated as SVV KS15-01(GenBank accession No. KX019804). The isolated virus was cultured on PK-

15 cells. Recombinant viruses, vKS15-01-Clone and vKS15-01-EGFP, were rescued from transfected BHK-21 cells and passaged on PK-15 cells (see details below). For both wild-type and recombinant viruses, the passage two viruses on PK-15 cells were used for subsequent *in vitro* and *in vivo* experiments.

Construction of full-length cDNA clones of SVV KS15-01

In order to construct a full-length cDNA clone, the SVV KS15-01 was re-sequenced using Sanger sequencing method. A set of primers was designed based on the conserved genomic regions of a Canadian virus strain (GenBank accession No. KC667560; Table 3). These primers were used in RT-PCR to amplify viral RNA genome of KS15-01 virus. The PCR products were sequenced at Eurofin MWG Operon sequencing facility (Louisville, KY). The 5'- and 3'-end genomic sequences were further determined using GeneRacer® core Kit (Invitrogen, Carlsbad, CA) with specific primers (Table 3). To construct a full-length cDNA clone, five separate fragments, named A to E, flanked with unique enzyme restriction sites were amplified using Pfu Ultra High-fidelity DNA Polymerase (Agilent, Santa Clara, CA) and assembled together. As shown in Figure 2-1, a cytomegalovirus (CMV) promoter was inserted upstream of the fragment A, while a hepatitis delta virus ribozyme element was incorporated at the 3'-terminus of the viral genome, following the fragment E. Initially, a stuffer fragment that contains the multiple cloning sites, fragment E, poly (A) tail and a hepatitis delta virus (HDV) ribozyme was synthesized and inserted into pACYC177 vector (Table 3). Fragments A was cloned into the modified vector through a standard DNA cloning procedure using SphI/SacI restriction enzyme sites. Subsequently, fragments B, C, and D were assembled into pACYC177 vector with fragments A and E using DNA recombination

method following the instruction of NEBuilder® HiFi DNA Assembly Cloning Kit (New England BioLabs, Ipswich, MA). To create a molecular marker for differentiating cloned virus from parental virus KS15-01, a SacI site ($_{4213}$GAGCTC$_{4218}$) was inactivated with C$_{4216}$ to T$_{4216}$ mutation using overlap extension PCR method as described previously (Ho et al., 1989). The resulting full-length cDNA clone was designated as pKS15-01-Clone (GenBank accession No. KX349733). To construct a full-length cDNA clone expressing EGFP, the EGFP gene (GenBank accession #U55762; Clontech Laboratories) was synthesized and fused with a Teschovirus 2A element (T2A) at its C-terminus. The EGFP-T2A fusion gene was inserted between the SVV genes 2A and 2B using overlap extension PCR method (Ho et al., 1989). This full-length cDNA clone was designated as pKS15-01-EGFP (GenBank accession No. KX349734).

Recovery of recombinant viruses

BHK-21 cells seeded in 6-well plate were transfected with a plasmid DNA of the full-length cDNA clone pKS15-01-Clone or pKS15-01-EGFP. Transfection was conducted using Lipofectamine 3000 reagent following the manufacturer's instructions (Invitrogen, Carlsbad, CA). At 48 h post-transfection, cell culture supernatant from BHK-21 cells was transferred to PK-15 cells. Cytopathic effect (CPE) was monitored daily after infection. Recombinant viruses were harvested during 18-48 h post infection (hpi) when significant CPE was observed. The cloned virus recovered from cDNA infectious clone, pKS15-01-Clone, was designated as vKS15-01-Clone, while the EGFP-tagged virus recovered from cDNA infectious clone, pKS15-01-EGFP, was designated as vKS15-01-EGFP.

Identification of recombinant viruses

To confirm the presence of the molecular marker (C_{4216} to T_{4216} mutation in SacI site) in the cloned virus, vKS15-01-Clone, RT-PCR was performed to amplify the genomic region (nt 3551-5227) containing the specific mutation. Initially, viral RNA was extracted from passage two of vKS15-01-Clone virus using the QIAamp viral RNA mini kit (Qiagen, Valencia, CA) following the manufacturer's instructions. After RNA extraction, cDNA was generated with Superscript III reverse transcriptase (Invitrogen, Carlsbad, CA), and the corresponding viral genomic region was amplified by PCR using the primer pair, SVV-3547F/SVV-5200R (Table 3). PCR product was gel-purified and digested by SacI, and was also subjected to DNA sequencing to confirm the presence of the C_{4216} to T_{4216} mutation. To confirm the presence of EGFP insertion in vKS15-01-EGFP virus, the corresponding viral genomic region (nt 3242-3700) was amplified by RT-PCR using the primer pair, SVV-6757F and SVV-7191R (Table 3), and PCR product was submitted for DNA sequencing (GenScript sequencing facility, Piscataway, NJ).

Monoclonal antibody (mAb) production

Antigens for production of mAbs to SVV VP1 and VP2 were expressed as recombinant proteins based on the sequence of SVV KS15-01. The VP1 and VP2-coding regions were amplified by RT-PCR from genomic RNA of KS15-01 virus, and the PCR products were cloned into the pET-28a (+) vector (Novagen, Madison, WI). Recombinant proteins were expressed and purified as described previously (Brown et al., 2009). The mAb135-48 (anti-VP1) and mAb30-158 (anti-VP2) were generated by immunizing BALB/c mice with VP1 and VP2 antigens, respectively. Detailed experimental procedures for mAb production were described

previously (Li et al., 2012; Rowland et al., 2005). Briefly, in order to successfully produce monoclonal antibodies against VP1 or VP2, proper primers with protective bases added were designed based on the gene sequence. Clone this gene into plasmid, transform to E.coli competent cells. After positive plasmid verification, clone into BL21 cells for protein expression. After two steps purification, proteins are concentrated. Mice were immunized with purified proteins mixed in adjuvant for several times. Meanwhile, ELISA and IFA were employed to detect antibodies in the serum. Next, myeloma cells were fused with mice splenic cells by using polyethylene glycol (PEG). Then spread fused cells onto plates, perform IFA or ELISA to screen monoclonal antibodies in the supernatant. Cell culture medium used here contains HAT (hypoxanthine-aminopterin-thymine), which can sustain only HGPRT(an enzyme involved in synthesis of nucleotides from hypoxanthine) positive cells. The myeloma cells are HGPRT negative and the B cells are HGPRT positive. Myeloma cells that fuse with another myeloma cell or do not fuse at all die in the HAT medium since they are HGPRT negative. The B cells that fuse with another B cell or do not fuse at all die because of lacking the capacity to divide indefinitely. Thus only hybridomas between B cells and myeloma cells can survive, being both HGPRT positive and cancerous. After several rounds of subcloning, hybridoma cells secreting antibodies against VP1 or VP2 are expandly cultured. After obtain ascites produced by immunizing mice with hybridoma cells, subclass of Ig was determined.

Western blot analysis

PK-15 cells in a 6-well plate were infected at a multiplicity of infection (MOI) of 0.01 with SVV KS15-01, vKS15-01-Clone, or vKS15-01-EGFP, or mock-infected. At 18 hpi, cell lysates were harvested with 200 μl/well Pierce™ IP Lysis Buffer (Pierce, Rockford, IL). After

centrifugation at 15000 g for 15 min, cell debris was removed. The cell lysate was mixed with 4x Laemmli loading buffer (Bio-Rad, Hercules, CA) containing 5% β-mercaptoethanol and denatured at 95 °C for 6 min. Proteins were separated on a 12.5% SDS-PAGE gel, and blotted onto nitrocellulose membrane. The membrane was blocked with 5% skim milk in 1x phosphate-buffered saline (PBS) at 4 °C overnight. To detect the expression of SVV VP1 and housekeeping gene encoding β-tubulin, the membrane was incubated at room temperature with a mixture of primary antibodies, including a mAb against VP1 (mAb135-48) and an anti-β-tubulin rabbit polyclonal antibody (abm, Canada). To detect the expression of EGFP and housing keeping gene encoding β-tubulin, a mixture of primary antibodies of anti-EGFP (Sigma-Aldrich, St. Louis, MO) and anti-β-tubulin was used. Antibodies were diluted with 1x PBS supplemented with 0.1% Tween 20 (PBST). After 1 h incubation, the membrane was washed with PBST three times, and then probed with secondary antibodies, IRDye® 680LT Donkey anti-Rabbit IgG (H + L) and IRDye® 800CW Donkey anti-Mouse IgG (H + L) (LI-COR Biosciences, Lincoln, NE). The membrane was incubated at room temperature for 1 h, and target proteins visualized using the Odyssey Fc Infrared Imaging System (LI-COR Biosciences, Lincoln, NE).

Immunofluorescence assay

PK-15 cells in a 12-well plate were infected with SVV KS15-01, vKS15-01-Clone, or vKS15-01-EGFP at an MOI of 0.01, or mock-infected. At 12 hpi, cell monolayers were fixed with 4% formaldehyde in PBS (pH 7.4) for 10 min, permeabilized with 0.1% Triton X-100. After 1 h incubation with primary anti-VP1 mAb135-48, cell monolayers were washed with PBS for three times and further incubated for 1 h with Alexa Fluor® 594 AffiniPure Donkey

Anti-Mouse IgG (H+L) (Jackson ImmunoResearch Inc., West Grove, PA) secondary antibody. After extensive washing, cells were analyzed under a fluorescent microscope, and pictures were taken with EVOS FL Cell Imaging System (Life technologies, Carlsbad, CA).

Virus growth kinetics and plaque forming assay

PK-15 cells at ~100% confluency in a 24-well culture plate were infected with SVV KS15-01, vKS15-01-Clone, or vKS15-01-EGFP at an MOI of 0.01, or mock-infected. After 1 h incubation, cell culture supernatant was removed and cell monolayer was washed with MEM. Fresh infection medium was then added. Cell culture supernatants were harvested at 6, 12, 24, 36, 48 hpi. The virus titer was measured by titration on PK-15 cells and results were reported as 50% tissue culture infective doses per milliliter ($TCID_{50}$/ml) according to the method of Reed and Muench (Reed and Muench, 1938). Plaque assays were performed using PK-15 cells as described previously (Fang et al., 2006).

Animal study

The pig experiment was performed according to protocols approved by the Institutional Animal Care and Use Committees (IACUC) of Kansas State University and Midwest Veterinary Service, Inc. (MVS). A total of eighteen 3-week-old pigs were housed at the large animal facility of MVS (Oakland, NE). Pigs were randomly assigned into four groups, with group 1 pigs (n=5) infected with the SVV KS15-01, group 2 pigs (n=5) infected with the vKS15-01-Clone virus, group 3 pigs (n=5) infected with the vKS15-01-EGFP virus, and group 4 pigs (n=3) were mock-infected with cell culture medium. Pigs were intranasally inoculated with 5 ml/pig of the virus (or culture medium) at a dose of $1x10^8$ $TCID_{50}$/ml. Clinical observations and rectal temperatures were recorded daily from 0-14 days post

infection (dpi). Serum, oral fluid, nasal swab and fecal swab samples were collected at 0, 3, 7 and 14 dpi. The pig experiment was terminated at 14 dpi. During necropsy, gross pathology for each pig was evaluated and abnormal tissue and skin samples were collected.

Quantitative RT-PCR

To evaluate viral load in serum, fecal swab, nasal swab and oral fluid samples, SVV quantitative RT-PCR (qRT-PCR) was performed by Kansas Veterinary Diagnostic Laboratory (KSVDL). Briefly, viral genomic RNA was prepared using a MagMAX-96 viral RNA isolation kit (Life Technologies, Carlsbad, CA) according to the manufacturer's instructions. Subsequently, qRT-PCR was performed using Path-ID™ Multiplex One-Step RT-PCR Kit (Applied Biosystems, Foster City, CA) in the CFX96 Touch Real-Time PCR Detection System with the following cycling parameters: 48 °C for 10 min, 95 °C for 10 min, 45 cycles of 95 °C for 15 sec and 60 °C for 60 sec. A standard curve was established by using serial 10-fold diluted KS15-01 virus from $1x10^6$ $TCID_{50}$/ml to $1x10^1$ $TCID_{50}$/ml. Viral RNA load equivalent to $TCID_{50}$/ml was determined based on the standard curve.

Neutralizing antibody assay

Serum neutralizing antibody assays were performed using the parental virus SVV KS15-01, and the neutralizing antibody titer was determined by immunofluorescence focus assay. Briefly, serum samples were heat-inactivated at 56 ºC for 30 min, and then 2-fold serially diluted with MEM containing 2% horse serum (HS). The diluted serum (100µl/well) was mixed with equal volume of KS15-01 virus (200 $TCID_{50}$) and incubated at 37 °C. After 1 h incubation, 150 µl of the serum-virus mixture was added to a 96-well microtiter plate containing 90-100% confluent PK-15 cells and incubated at 37 °C. At 18 hpi, cells were fixed

using ice cold methanol at -20 °C for 30 min. Fixed cells were stained with VP2 specific mAb30-158, and Alexa Fluor® 488 AffiniPure goat anti-mouse IgG (H+L) (Jackson ImmunoResearch Inc., West Grove, PA) was used as a secondary antibody. Cells in each individual wells were examined using EVOS FL Cell Imaging System (Life technologies, Carlsbad, CA). The neutralizing antibody titer was defined as the highest serum dilution at which more than 90% of virus growth was inhibited.

SVV specific antibody response

Indirect immunofluorescence assays were performed to assess SVV specific antibody response in serum samples from pigs inoculated with parental virus and recombinant viruses, or mock infected. Briefly, PK-15 cells with 100% confluency in 96-well plate were infected with KS15-01 virus at an MOI of 0.01, and fixed with ice-cold methanol at -20 °C for 30 min. Fixed cells were incubated with 2-fold serially diluted pig serum samples with the first dilution of 1:5. After 1 h incubation at 37 °C, the cell monolayers were washed three times with PBS, and then incubated with FITC conjugated secondary antibodies mixture of Goat anti-Porcine IgM Secondary Antibody, Goat anti-Porcine IgA Secondary Antibody, and Goat anti-Porcine IgG Secondary Antibody (Novus Biologicals, Littleton, CO) at a dilution of 1:200. After three times wash with PBS, cells in each individual wells were examined using EVOS FL Cell Imaging System (Life technologies, Carlsbad, CA). SVV specific antibody titer was defined as the highest serum dilution at which SVV proteins were detected.

Analysis of swine cytokine response

The expression levels of IFN-α and IFN-γ in serum samples were determined using ProcartaPlex Porcine IFN alpha Simplex kit and ProcartaPlex Porcine IFN gamma Simplex

kit (eBioscience, San Diego, CA) following the manufacturer's instructions.

Statistical analysis

Statistical analyses were performed by using one-way analysis of variance (ANOVA) followed by Tukey's *post hoc* test using GraphPad InStat Prism software (version 5.0) to establish variations between the indicated pig groups. Statistical significance was assessed at *P* values of less than 0.05, 0.01, or 0.001.

Results

Construction of an infectious clone of emerging Seneca Valley Virus isolate KS15-01

In order to construct a cDNA clone, the full-length genome sequence of SVV KS15-01 isolate was obtained (GenBank accession number KX019804). Sequence comparisons result showed that the complete genome sequence of SVV KS15-01 shared a 93.9%~99.4% nucleotide sequence identity to nine complete SVV genomes in GenBank (as of March 17, 2016). Phylogenetic analysis showed that the SVV KS15-01 is closely related to the recently reported US and Brazilian strains (Zhang et al., 2015) (data not shown).

With the availability of the complete genome sequence of SVV KS15-01, a full-length genomic cDNA clone of the virus (pKS15-01-Clone) was constructed using the strategy shown in Figure 2-1. This pKS15-01-Clone construct contains a CMV promoter at the 5' terminus of the viral genome, the 7281-nucleotide full-length genome of SVV KS15-01, and a poly(A) tail of 22 residues incorporated at the 3' end of the genome. Compared to the genome sequence of the parental virus, the DNA sequence of pKS15-01-Clone contained 4 nucleotide differences (Table 1), including an additional T at the 5' end, a G_7 to T_7 mutation

at the 5' UTR, T_{7234} to C_{7234} and C_{7262} to T_{7262} mutations at the 3' UTR; a mutation at nucleotide C_{4216} to T_{4216} was introduced to inactivate the SacI restriction enzyme site in 2C region for differentiating the cloned virus from the parental virus (Figure 2-2A-B). The C_{4216} to T_{4216} mutation is a silent mutation with no change on the encoded amino acid sequence.

In vitro recovery and characterization of recombinant virus derived from Seneca Valley Virus full-length cDNA clone pKS15-01-Clone

To rescue the cloned virus, plasmid DNA of pKS15-01-Clone was transfected into BHK-21 cells, and cell culture supernatant from the transfected cells were passaged onto PK-15 cells at 48 h post-transfection. At 12 hpi, PK-15 cells were stained using the VP2-specific mAb 30-158 (Figure 2-3A). The results showed that the VP2 protein was specifically detected in PK-15 cells inoculated with the cell culture supernatant from transfected BHK-21 cells. Upon further passage onto fresh PK-15 cells (passage two on PK-15 cells), cytopathic effects were observed within 18 to 48 hpi. The passage two viruses collected from PK-15 cells showed an average titer of $1x10^8$ $TCID_{50}$/ml. These results demonstrated that the viable cloned virus (vKS15-01-Clone) was recovered from the full-length cDNA infectious clone pKS15-01-Clone.

The growth kinetics of the vKS15-01-Clone virus and parental virus SVV KS15-01 were compared. PK-15 cells were infected with each of the viruses at an MOI of 0.01 and harvested at 6, 12, 24, 36, 48 hpi. The results showed that the cloned virus possessed growth kinetics similar to the parental virus (Figure 2-4A). The peak viral titers reached at 36 hpi for both viruses, in which the peak titer of the cloned virus was $10^{8.0}$ $TCID_{50}$/ml, while the peak titer of the parental virus was $10^{8.4}$ $TCID_{50}$/ml. Plaque morphology of these viruses was

further determined. As shown in Figure 2-4B, the plaque size produced by the cloned virus was similar to that of the parental virus. These results indicate that the cloned virus possesses *in vitro* growth properties similar to those of the parental virus.

To differentiate the cloned virus from the parental virus, a SacI restriction enzyme site was inactivated in 2C region (Figure 2-1). As shown in Figure 2-2A, a 1677-bp RT-PCR fragment derived from amplifying nucleotides 3551 to 5227 of the viral genome was cleaved by SacI in the parental virus. In contrast, the corresponding RT-PCR product amplified from the cloned virus was not cleaved by SacI.

Seneca Valley Virus infectious clone as a vector for expressing EGFP

With the availability of this infectious clone, we further explored its potential in expressing a reporter gene. A synthetic gene encoding an EGFP and teschovirus 2A peptide (T2A) fusion protein was cloned into the 2A/2B junction of pKS15-01 backbone, generating the plasmid, pKS15-01-EGFP (Figure 2-1). The T2A is a "self-cleaving" peptide allowing highly efficient cleavage between genes upstream and downstream of the 2A peptide. This construct allows ribosome skipping events occurring at the SVV 2A and the engineered T2A regions during translation of SVV polyprotein, leading to release EGFP-2A protein without affecting the functions of other SVV proteins.

The plasmid, pKS15-01-EGFP, was transfected into BHK-21 cells, and the cell culture supernatant from transfected BHK-21 cells was passaged onto PK-15 cells at 48 h post-transfection. The live EGFP-expressing cells were visible as early as 6 hpi (Figure 2-3A). To confirm the expression of viral proteins, at 12 hpi, cells were fixed and stained with anti-VP1 mAb 135-48. An Alexa Fluor® 594 AffiniPure Donkey Anti-mouse IgG (H+L)

antibody was used as the secondary antibody. Immunofluorescent microscopy showed the expression of both EGFP and VP1 proteins (Figure 2-3A). To determine if the expression of EGFP affected virus replication, the growth kinetics of the EGFP-tagged virus (vKS15-01-EGFP) was compared to those of the parental wild-type and cloned viruses. The vKS15-01-GFP displayed a similar growth behavior as the parental virus SVV KS15-01 and cloned virus vKS15-01-Clone (Figure 2-4A-B). To determine the stability of the EGFP gene at the insertion site, the genomic region containing EGFP insertion of the passage two virus was sequenced. The results confirmed the existence of intact EGFP in vKS15-01-EGFP virus (Figure 2-2C). We further analyzed the expression of EGFP protein in vKS15-01-EGFP virus infected cells using western blot. The result confirmed the expression of EGFP (~27-kDa) and a cleaved VP1 (~32-kDa) in cells infected with vKS15-01-EGFP virus. In contrast, only VP1 (~32-kDa) was detected in cells infected with the parental virus SVV KS15-01 and cloned virus vKS15-01-Clone (Figure 2-3B).

Clinical observations in nursery pigs infected with the parental and recombinant Seneca Valley Virus

A total of eighteen 3-week-old pigs, divided into four groups, were infected with parental virus SVV KS15-01 (group 1, n=5), cloned virus vKS15-01-Clone (group 2, n=5), EGFP virus vKS15-01-EGFP (group 3, n=5), or mock-infected with cell culture medium (group 4, n=3). All pigs in group 1 and four of five pigs in group 2 developed clinical signs, including respiratory distress and/or lethargy (Figure 2-5B). Three pigs in group 1 and three pigs in group 2 had rectal temperature over 104^{o}F during the first 6 days post inoculation (Figure 2-5A). Fluid filled vesicles on the snout first appeared at dpi 1 on four pigs in group 1

(Figure 2-5C; Table 2). These vesicles progressed into ulcerative lesions and resolved in 3-4 days (Table 2). Gross ulcerative lesions on distal limbs, especially around the coronary bands, were also observed on two pigs in group 1, which first appeared at 7 dpi (Figure 2-5D; Table 2). In contrast, no apparent clinical signs were observed in group 3 and 4 pigs. Rectal temperatures were normal for all pigs in groups 3 and 4, except for one pig in group 3 whose temperature was over 104°F at 1, 2, and 14 dpi (Figure 2-5A). At 14 dpi, one pig from group 1 showed healing scars from the vesicular ulcers on the snout (Figure 2-5E); all five pigs from group 1 showed round, erosive lesions around the coronary bands of the lateral claws (Figure 2-5F), and lesions on any combination of legs with front leg injury being more common. In one of the group 3 pigs, a footpad erosive lesion was observed on the right front leg during necropsy, but no dorsal snout lesions and coronary band lesions were observed in this group. At necropsy (14 dpi), enlarged mesenteric lymph nodes were observed on two pigs in group 2. Mild lung lesions were observed in a total of seven pigs, including two pigs from group 1, three pigs from group 2, and three pigs from group 3. One pig from group 1 showed severe multifocal lung lesions, which was suspected to be associated with bacterial infection. Gross pathology was also performed on tonsil, heart, liver, spleen, kidney, and intestine; no gross lesion was observed on these internal organs from group 1-4 pigs.

In vivo growth properties of the parental and recombinant Seneca Valley Virus in pigs

Serum, nasal swab, oral fluid and fecal swab samples were collected to determine the level of viral replication/shedding in pigs. Infectious SVV was isolated from serum samples of group 1 and group 2 pigs at 3 dpi (data not shown), indicating active replication of SVV in

pigs. At 3 and 7 dpi, qRT-PCR results showed that SVV RNA was detected in all the samples from pigs of groups 1 and 2. A higher level of viral RNA was detected in serum and fecal samples from group 2 pigs at 3 dpi, but the amount of viral RNA reached the similar level for both groups of pigs at 7 dpi (Figure 2-6A-B). At 14 dpi, both groups almost cleared out of the viruses, in which minimal amounts of viral RNA were detected in serum, fecal and nasal swab sample (Figure 2-6A-C); however, a low level of viral RNA (equivalent to $10^{2.0}$ $TCID_{50}$/ml) still remained in the oral fluid samples (Figure 2-6D). In group 3 pigs, at 3 and 7 dpi, only one pig (#34) showed positive qRT-PCR result in the serum sample, but four out of five pigs showed positive qRT-PCR result in nasal swab, and all five pigs showed positive qRT-PCR result in oral fluid and fecal swab samples (Figure 2-6). At 14 dpi, viral RNA was not detected in serum and nasal swab samples, and only minimal amount (equivalent to $10^{0.91}$ $TCID_{50}$/ml) was detected in one of the fecal samples (Figure 2-6B). In comparison to those of groups 1 and 2 pigs, viral RNA levels were lower in all samples (except oral fluid at 14 dpi) from group 3 pigs; and some differences were statistically significant at 3 dpi in serum, nasal swab and fecal swab samples (Figure 2-6A-C), suggesting that the EGFP insertion impaired the *in vivo* growth ability of the virus. As expected, no SVV RNA was detected by qRT-PCR using samples from mock-infected group 4 pigs.

In vivo stability of mutations or insertions introduced in Seneca Valley Virus

As indicated above, to differentiate the cloned virus from the parental virus, we introduced a C to T mutation to inactive the SacI restriction enzyme site. To determine the stability of the SacI mutation in pigs, the corresponding region (nt 3551 - 5227) was amplified by RT-PCR using RNA extracted from serum samples of group 2 pigs. As a

comparison, serum samples from group 1 pigs were included in the analysis. The PCR product was subjected to DNA sequencing analysis. The result confirmed the presence of the SacI mutation in all five pigs from group 2, but not in any of the pigs from group 1. The PCR product was further verified by restriction enzyme digestion using SacI enzyme. As shown in Figure 2-7A, a 1677-bp PCR fragment derived from each of group 2 pigs was not cleaved by SacI; in contrast, the PCR fragment derived from the group 1 pigs was cleaved by SacI. The same method was used to verify the EGFP insertion in the virus from group 3 pigs. Initially, viral RNA from the serum of pig #34 (showed positive qRT-PCR result) was used to RT-PCR amplify the EGFP insertion region, and the PCR product was subjected to sequence analysis. The pair of primers was design to cover the 3487- 4472 nucleotide region of the viral genome. With the 720-bp EGFP insertion in this region, a 986-bp PCR product was expected. However, a PCR product close to 500 bp was obtained and the sequencing result revealed that the amino acids 63 to 237 of EGFP were deleted (Figure 2-7B and 2-7F). We further amplified the corresponding EGFP insertion region using viral RNA from oral fluid, nasal swab and fecal swab samples. Interestingly, a 986-bp PCR product was obtained from all of these samples except two nasal swab samples with very low viral loads ($10^{0.6}$ $TCID_{50}$/ml) and sequencing result confirmed the existence of full-length intact EGFP gene in the virus from each of the group 3 pigs (Figure 2-7C-E). In addition, a PCR product around 500 bp was also amplified from the fecal swab sample of pig #34, and the sequencing result indicated that the EGFP deletion was exactly the same as that from the serum sample.

Innate and adaptive immunity following infection with parental and recombinant Seneca Valley Virus

We further analyzed the host immune responses stimulated by the parental and recombinant viruses. Since IFN-α is an indicator of the early innate immune response, we measured IFN-α expression in serum samples from infected and control pigs through the time course of study. Overall, only minimal level of IFN-α was stimulated in all the pigs, and there was no significant difference on the IFN-α expression levels between different groups of pigs (Figure 2-8). At 3 dpi, mean IFN-α protein concentration was slightly higher in groups 1 pigs (9.8 pg/ml) and group 2 pigs (14.0 pg/ml), in comparison to that of group 3 pigs (1.8 pg/ml) and group 4 pigs (6.9 pg/ml) (Fig. 8B). However, these differences were not statistically significant. IFN-γ was un-detectable in all groups of pigs through the time course of the study. In contrast, SVV infection stimulated a rapid robust serum neutralizing (SN) antibody response (Figure 2-9). The SN antibody response was observed at 3 dpi in group 1 and group 2 pigs. At 7 and 14 dpi, the SN titer reached more than 1:2000 in some of the pigs from groups 1 and 2. The SN titers in group 3 pigs were consistently lower in comparison to these two groups. Among the five pigs in group 3, pig #34 consistently showed the highest SN titers with the titer of 1:256 at 7 dpi, and 1:1024 at 14 dpi. The SN titers of the other four pigs in group 3 were lower, but still 2-100-fold higher than those of mock-infected pigs. By using indirect immunofluorescence assay, we further assessed the dynamic production of SVV specific antibodies (IgA, IgM, and IgG) in serum samples through the time course of study. From 7 dpi, SVV specific antibodies were detected in serum samples from group 1, 2 and 3, but not from group 4 pigs (Figure 2-10). In comparison with recombinant viruses, parental

virus induced higher level of SVV specific antibodies at 7 dpi, although the differences were not statistically significant. However, at 14 dpi, the SVV specific antibodies in serum samples from group 1 and 2 pigs reached similar level.

Figures and Tables

Table 1. Nucleotide differences between the genome of parental virus SVV KS15-01 and full-length cDNA clone pKS15-01-Clone

Nucleotide position within SVV KS15-01 genome	Nucleotide in parental virus	Nucleotide in cDNA clone	Gene position
N/A	N/A	T	5’ UTR
7	G	T	5’ UTR
4216	C	T	2C
7234	T	C	3’ UTR
7262	C	T	3’ UTR

Table 2. Surface lesions on snout and coronary band of SVV KS15-01- infected pigs

	Pig #18
4 dpi	Ulcerative lesion 1cm x 1 cm medial portion of left snout
5 dpi	Ulcerative lesion 1cm x 1 cm on left snout
6 dpi	Ulcerative lesion 1cm x 1 cm on left snout
7 dpi	Snout lesion resolved
	Pig #22
1 dpi	0.5cm x 0.5cm focal spot of hyperemia on center of nose
2 dpi	1/2cm x 1/2cm area hyperemia, focal on nose
3 dpi	1/2cm x 1/2cm area of hyperemia on nose
4 dpi	Nose lesion has resolved
	Pig #24
7 dpi	Hyperemia of lateral side left + right front coronary bands
8 dpi	Ulcers on lateral toes of right & left coronary bands
9 dpi	Right & left front, both
11 dpi	Left front lateral claw, 1cm x 1cm ulcer, lateral carpus
12 dpi	Ulcer on left lateral claw, front leg
	Pig #28
7 dpi	Hyperemia of lateral right front coronary band
8 dpi	Ulcer on right front lateral toe coronary band
9 dpi	Right front lateral toe coronary band ulcer
10 dpi	Area of hyperemia right front lateral claw
13 dpi	0.5cm x 0.5cm ulcer on left tip of snout
	Pig #32
7 dpi	Snout ulcer
8 dpi	Snout ulcer
9 dpi	Snout ulcer
10 dpi	1/2cm x 1/2cm central dorsal part of snout
11 dpi	Snout lesions resolved

Table 3. Primers for constructing full-length cDNA clone and sequencing viral genome

Name	Sequence (5' to 3')	Anchor site[a]	Usage
SVV-F1	AGAGCTGCATGCTAATAGCTTTGAAATGGGGGGCTGGGCCCTCATG	4 ~ 22	Clone fragment A; Sequencing
SVV-R433	CACGTGGACTCTGTGTCGGAGCTTG	433 ~ 457	
SVV-311F	GCGGAAAGCGCTGTAACCACATGC	311 ~ 334	Clone fragment B; Sequencing
SVV-2303R	CAAAATGTCAGAGTGATTTGGATACACC	2303 ~ 2330	
SVV-2211F	GCCTCTCATCTCCTTCCCGATCAC	2211 ~ 2234	Sequencing
SVV-4160R	GAGACTTTGGGCCAAATTAGTCTTCC	4160 ~ 4185	Sequencing
SVV-3547F	GATCTAGTCACTCTGGCCTCTCTC	3547 ~ 3570	Sequencing
SVV-5200R	GACCGCAGCCTCAAAGCCCATGTC	5200 ~ 5223	Sequencing
SVV-2211F	GCCTCTCATCTCCTTCCCGATCAC	2211 ~ 2234	Clone fragment C; Sequencing
SVV-5200R	GACCGCAGCCTCAAAGCCCATGTC	5200 ~ 5223	
SVV-4982F	CCAAGCTAGGTCTTGCCCTAGCTG	4982 ~ 5005	Sequencing
SVV-6810R	CCAGAAGGTCGTCACCGTAGGCGATG	6810 ~ 6835	Sequencing
SVV-6661F	GCTTACGGCGAGCGTCGCATCAAG	6661 ~ 6684	Sequencing
SVV-7236R	TGAGTTCTCCCAGAATCGCCGGCAG	7236 ~ 7260	Sequencing
SVV-4982F	CCAAGCTAGGTCTTGCCCTAGCTG	4982 ~ 5005	Clone fragment D; Sequencing
SVV-7236R	TGAGTTCTCCCAGAATCGCCGGCAG	7236 ~ 7260	
SVV-891F	CGAACTACAGGGTAATGTTCAGAC	891 ~ 914	Sequencing
SVV-2810F	GAATGTAATTAAGGTACTGGAGAAG	2811 ~ 2835	Sequencing
SVV-4700R	GTCCACGAAGGGCACATGGGCAGC	4705 ~ 4728	Sequencing
SVV-5520F	AACTCCCGTGTGGTTGGCGTTTCG	5521 ~ 5544	Sequencing
SVV-130R	TGCGCTAACACCTTTGGCGACGCAG	130 ~ 154	5' RACE
SVV-7075F	CTGCAATCTGTTTCTATGTTGGCTCAAC	7075 ~ 7102	3' RACE
SVV-5051F	CCCTTGATGTCAAACCTGACGGCAAG	1532 ~ 1557	Construct pKS15-01-EGFP
SVV-7000R	AGGGCCAGGGTTGGTCTCGACGT	3482 ~ 3504	Construct pKS15-01-EGFP
EGFP-F	ACGTCGAGACCAACCCTGGCCCTATGGTGAGCAAGGGCGAGGAG	N/A	Construct pKS15-01-EGFP
T2A-R1	CAAGATCGGGTTGTCAGAAGCAGGTCCGGGGTTCTCTTCCA	N/A	Construct pKS15-01-EGFP
T2A-R2	CAAGATCGGGTTGTCAGAAGCAGGTCCGGGGTTCTCTTCCA	N/A	Construct pKS15-01-EGFP
SVV-7021F	CCTGCTTCTGACAACCCGATCTTG	3502 ~ 3525	Construct pKS15-01-EGFP
SVV-9470R	CTGGGATCAAATTTTGACAACACAG	5927 ~ 5951	Construct pKS15-01-EGFP
SVV-6757F	TCTGTCTCTTCCGTGCTTCCCGTG	3238 ~ 3261	Verify EGFP insertion
SVV-7191R	GTTAGATAGCGTGGCGGCCAAGGC	3673 ~ 3696	Verify EGFP insertion
SVV-7351F	CTGATGACCAAGCCCTCCGTGAAG	3832 ~ 3855	Mutate SacI in 2C region
SVV-7710R	GTTCGACTCGTTGGGCGGAACTCTGCTTGGCATTGATCAT	4192 - 4231	Mutate SacI in 2C region
SVV-7710F	ATGATCAATGCCAAGCAGAGTTCCGCCCAACGAGTCGAAC	4192 - 4231	Mutate SacI in 2C region
SVV-8680R	ATTTCCATAAGAGAGAGCGCTCC	5161 ~ 5183	Mutate SacI in 2C region
Stuffer fragment	TACTATGCATGCCTACATGAGCTCCATTGCGCATCTCCTAGGATCAT TGGGACCTACTATCTGTACATAGTAT[b]CTGCAGGCAAGATGGAGGG CCTTGTTCGACTGACCTAGATAGCCCAACGCGCTCCGGTGCTGCCG GCGATTCTGGGAGAACTCAGTCGGAACAGAAAAGGG[c]AAAAAAA	N/A	Creating multiple cloning site for assembly of viral genome

	AAAAAAAAAAAAAAAAAAAAAAGGCCGGCATGGTCCCAGCCTC CTCGCTGGCGCCGGCTGGGCAACATTCCGAGGGGACCGTCCCCTC GGTAATGGCGAATGGGAC[d]TCTAGATTAGTC		

a: The primer anchor sites on the reference virus genome (GenBank accession No. KC667560).

b: The multiple cloning sites used for cloning virus genomic fragments.

c: E fragment of virus genome as showed in figure 1A.

d: The hepatitis delta virus ribozyme immediately following 3' end of virus genome.

N/A: not applicable.

Table 4. Daily clinical observation from dpi 0 to dpi 14

	Parental virus					Cloned virus					EGFP virus					Mock		
Pig # / DPI	18	22	24	28	32	1	2	5	10	19	20	30	33	34	35	21	25	29
0	0	0	0	0	0	0	0	0	0	0	0	0	0	0	0	0	0	0
1	0	1	0	0	0	0	0	0	0	0	0	0	0	0	0	0	0	0
2	0	2	0	0	0	0	1	1	0	0	0	0	0	0	0	0	0	0
3	0	3	2	2	1	1	1	2	3	0	0	0	0	0	0	0	0	0
4	3	0	1	2	0	0	1	1	1	0	0	0	0	0	0	0	0	0
5	3	0	2	2	0	0	1	1	0	0	0	0	0	0	0	0	0	0
6	3	0	2	2	0	0	1	1	0	0	0	0	0	0	0	0	0	0
7	0	0	4	2	3	0	1	2	0	0	0	0	0	0	0	0	0	0
8	1	0	6	3	3	0	0	1	0	0	0	0	0	0	0	0	0	0
9	1	1	7	3	3	0	1	3	0	0	0	0	0	0	0	0	0	0
10	0	0	0	3	3	1	0	1	0	0	0	0	0	0	0	0	0	0
11	0	0	4	0	0	2	0	0	0	0	0	0	0	0	0	0	0	0
12	1	0	5	0	0	2	1	0	0	0	0	0	0	0	0	0	0	0
13	1	0	0	3	0	0	0	0	0	0	0	0	0	0	0	0	0	0
14	0	0	0	0	0	0	0	0	0	0	1	0	0	0	0	0	0	0

The total score was calculated by adding below individual scores together.

Attitude score. 0, normal; 1, mildly depressed; 2, moderately depressed; 3, moribund.

Respiratory score. 0, normal; 1, mildly abnormal respiratory character; 2, severely abnormal respiratory character (eg: dyspnea).

Abdominal appearance score. 0, normal; 1, gaunt.

Surface lesion score on snout, oral mucosa and coronary band. 0, normal surfaces; 1, hyperemia; 2, blister (vesicle formation); 3, ulcerative lesion.

Table 5. Rectal temperature record from dpi 0 to dpi 14

	Parental virus (Group 1)					**Cloned virus (Group 2)**					**EGFP virus (Group 3)**					**Mock (Group 4)**		
dpi	18	22	24	28	32	1	2	5	10	19	20	30	33	34	35	21	25	29
0	102.1[a]	102.5	103	102.9	102.5	101.1	102.3	102.4	101.5	102.9	102.4	101.8	102.7	102.3	101	102.1	103	102.4
1	103.4	103.4	103.5	103.1	102.7	103.1	102.4	103.9	103	103.3	105.2	102.3	102.6	104.1	103.6	101.8	102.2	102.2
2	103.7	104.9	103.4	103.3	102.8	102.6	105.4	105.7	103.3	103	104.5	103.1	102.8	103.5	103.1	102.3	103.3	103
3	104	104	104.4	103.7	102.7	103.4	105	107	103.1	102.9	102.6	102.9	103.6	103.6	103.1	102	103.7	102.6
4	104.1	104.4	105.6	103.1	103.3	103.8	103.2	103.6	103.6	105	103.9	103	103.3	103.2	102.7	101.9	103.1	102.3
5	104.6	104.5	106.3	104.3	104.2	102	103.9	104.1	103	103.6	103.3	102.9	102.9	103.4	102.8	102.5	102.7	103
6	104.8	104.7	104.1	103.2	103.7	102.8	103.6	104.1	103.2	103.7	102.2	103.7	102.9	104.2	102.9	102.6	102.6	102.3
7	103.8	104	103.7	103.2	103.4	103.3	103.5	103.5	103.3	103.7	102.4	103.1	102.3	103.3	102.8	103	102.5	102.1
8	103.8	103.9	103.6	103.4	104.4	102.9	103.8	102.8	103.2	102.4	103.1	102.9	103	102.7	103.2	102.5	103.1	103
9	104.2	103.6	104.2	103.6	103.4	102	104	103.2	103.6	103.7	102.1	103.6	103.2	103	103.3	102.2	102.8	103.7
10	104	103.6	103.2	103.4	104.1	103.1	103.5	104.6	103.7	103.4	103.1	103.3	103.5	103.3	102.6	103.4	103	103.1
11	103.9	103.1	103.9	103.3	103.6	104.4	103.4	102.6	102.9	103.2	103.2	102.8	102.8	103.3	103.4	103	103.3	102.2
12	104.4	104.3	103.6	103.8	104.1	104.3	104.8	103.1	102.4	103.1	102.7	104	103	102.5	102.9	102.4	102.2	103.4
13	104.6	104.2	104.2	104.3	103.8	103	103.1	103.1	102.7	103.5	103.5	103	102.8	103.5	102.8	103.3	103	102.7
14	103	103.2	103.2	103.2	103.6	102	103.7	103.4	102.9	103.3	105.4	102.8	102.8	103.1	102.4	102.4	102.9	103.2

a: temperature in Fahrenheit (°F).

Figure 2-1. Schematic diagram of the full-length SVV genome and construction of the full-length cDNA clones.

(**A**) SVV genome organization and strategies of assembling the full-length cDNA clone. Top scheme: Genome organization of SVV. The ORFs are flanked by 5' and 3' UTR followed by poly(A) tails at the 3' end. Arrows indicate the polyprotein processing site by 3C protease. Dotted red line showing the SacI restriction enzyme site for introducing the mutation in cloned virus in panel B. Bottom scheme: Five separate genomic fragments were amplified and assembled into the pACYC177 vector using the unique restriction enzyme sites and Giboson assembly cloning method (see details in Materials and Methods section). The full-length viral genome is under the control of a CMV promoter and followed by a HDV ribozyme. (**B**) Genome organization of the cloned virus vKS15-01-Clone with SacI site inactivated in 2C region. (**C**) A scheme of the reporter virus genome with an EGFP-T2A fusion gene inserted between 2A and 2B. T2A: teschovirus 2A peptide.

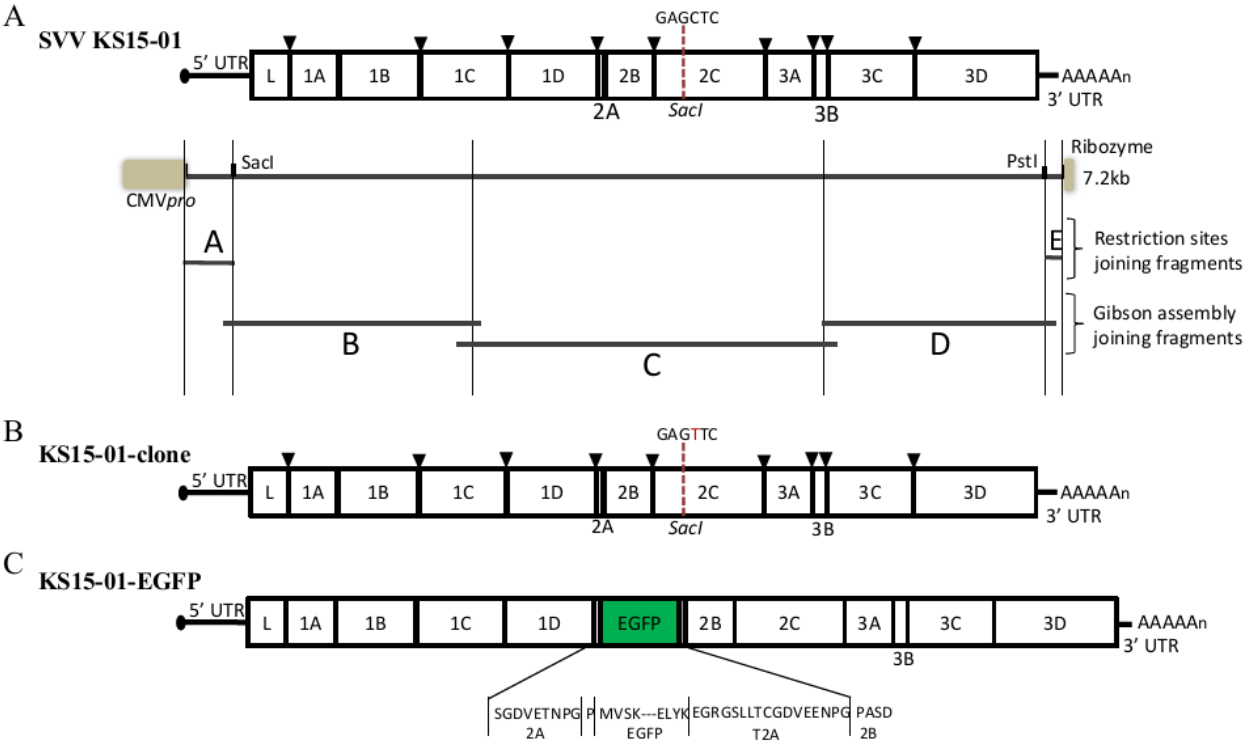

Figure 2-2. Differentiation of the parental virus from the cloned virus and EGFP-tagged virus in infected cells.

(**A**) Agarose gel picture showing the SacI enzyme digested DNA fragments generated by RT-PCR amplification of viral genomic region nt 3551-5227 from the SVV KS15-01 (parental virus) and vKS15-01-Clone (cloned virus). (**B**) DNA sequencing result of PCR products generated in panel A. Gray box showing the SacI enzyme site being mutated (C_{350} to T_{350}) in the cloned virus. (**C**) Agarose gel picture showing the DNA fragments generated by RT-PCR amplification of the viral genomic region containing the EGFP insertion site.

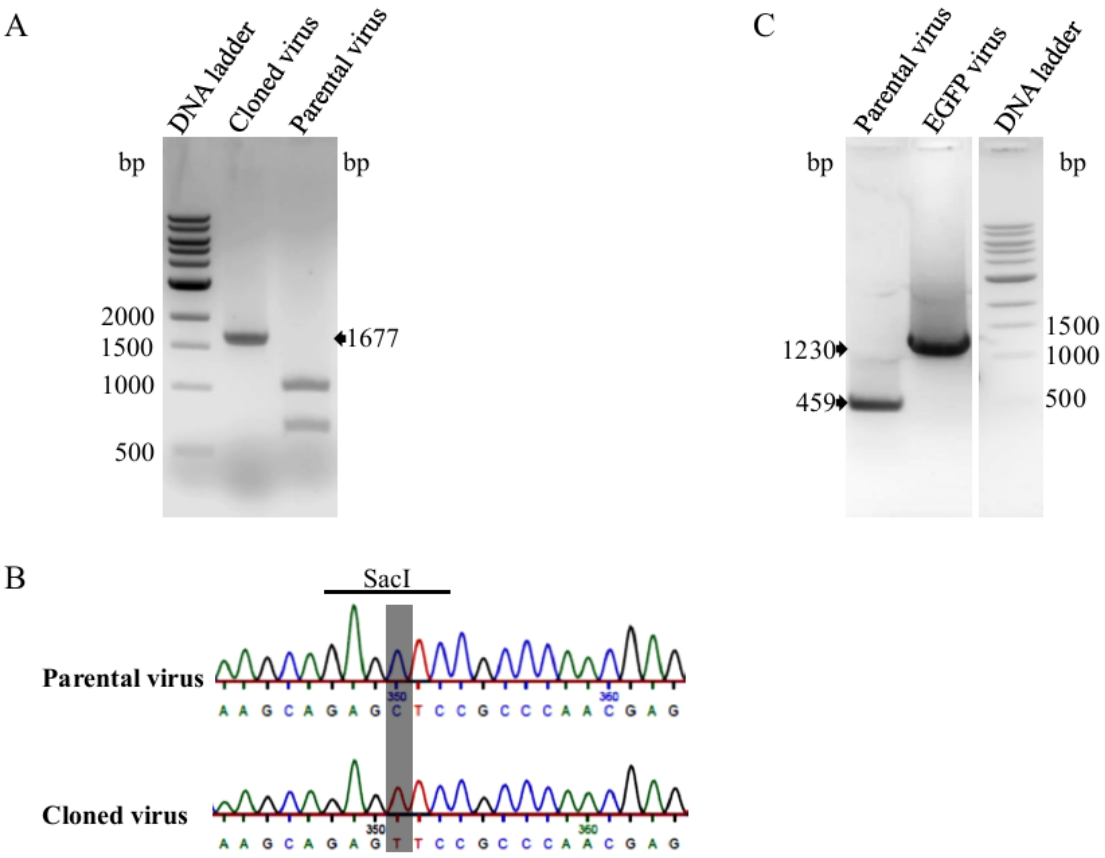

Figure 2-3. Detection of the viral protein and EGFP expression in parental and recombinant virus- infected cells.

(**A**) Immunofluorescent assay for detecting SVV VP1 and EGFP expression. PK-15 cells were infected with SVV KS15-01 (parental virus), vKS15-01-Clone (cloned virus) or vKS15-01-EGFP (EGFP virus) at an MOI of 0.01; mock-infected cells (PK-15) were used as the negative control. At 12 hpi, cell monolayers were fixed and stained with anti-VP1 mAb. The SVV VP1 was labeled red fluorescence and EGFP was shown as green fluorescence. Cell nucleus DNA was stained by DAPI (blue). (**B**) Western blot analysis of VP1 and EGFP expression. Cell lysates from PK-15 cells infected with SVV KS15-01 (parental virus), vKS15-01-Clone (cloned virus) vKS15-01-EGFP (EGFP virus), or mock-infected cells (PK-15) were harvested at 18 hpi and subjected to western blot analysis using mAbs against VP1 and EGFP. The expression of housekeeping gene β-tubulin was detected as a loading control.

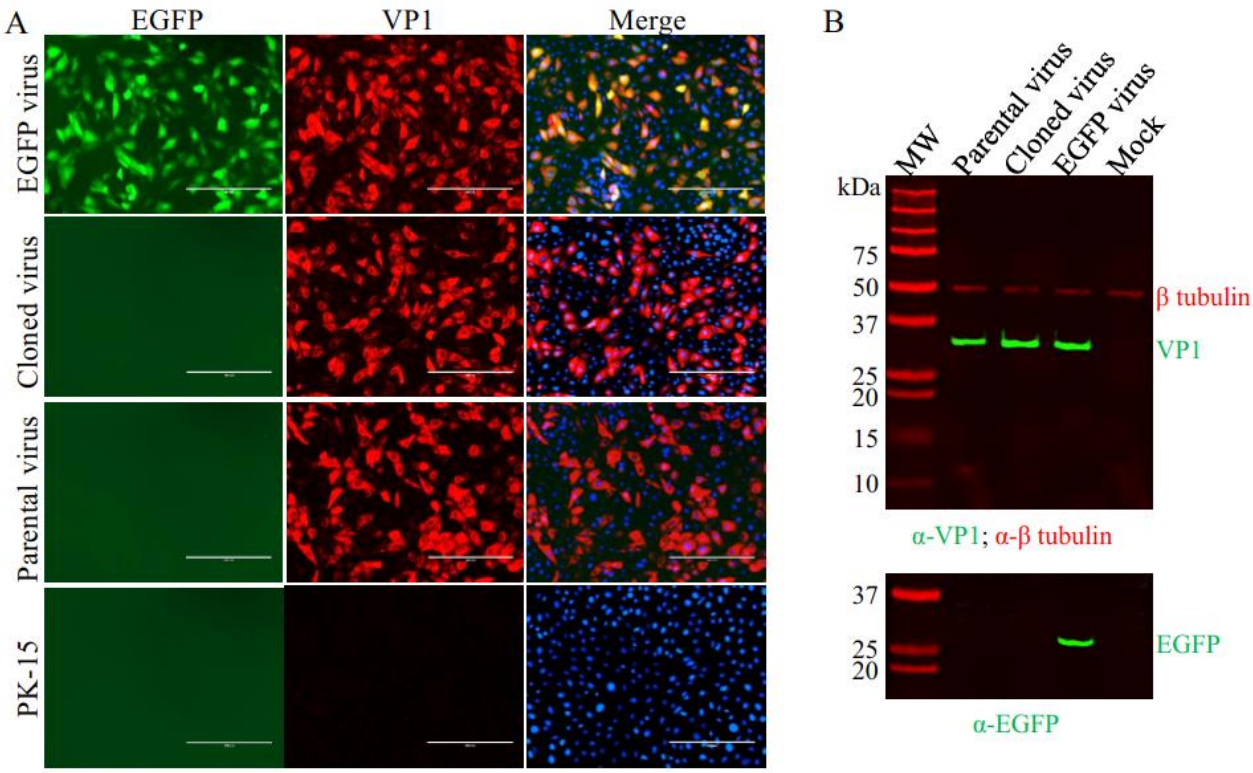

Figure 2-4. *In vitro* growth characterization of the parental and recombinant viruses. (**A**) Multiple-step virus growth curve. Each data point shown represents the mean value from duplicates, and error bars show standard errors of the mean (SEM). (**B**) Plaque morphology of SVV KS15-01 (parental virus), vKS15-01-Clone (cloned virus) vKS15-01-EGFP (EGFP virus).

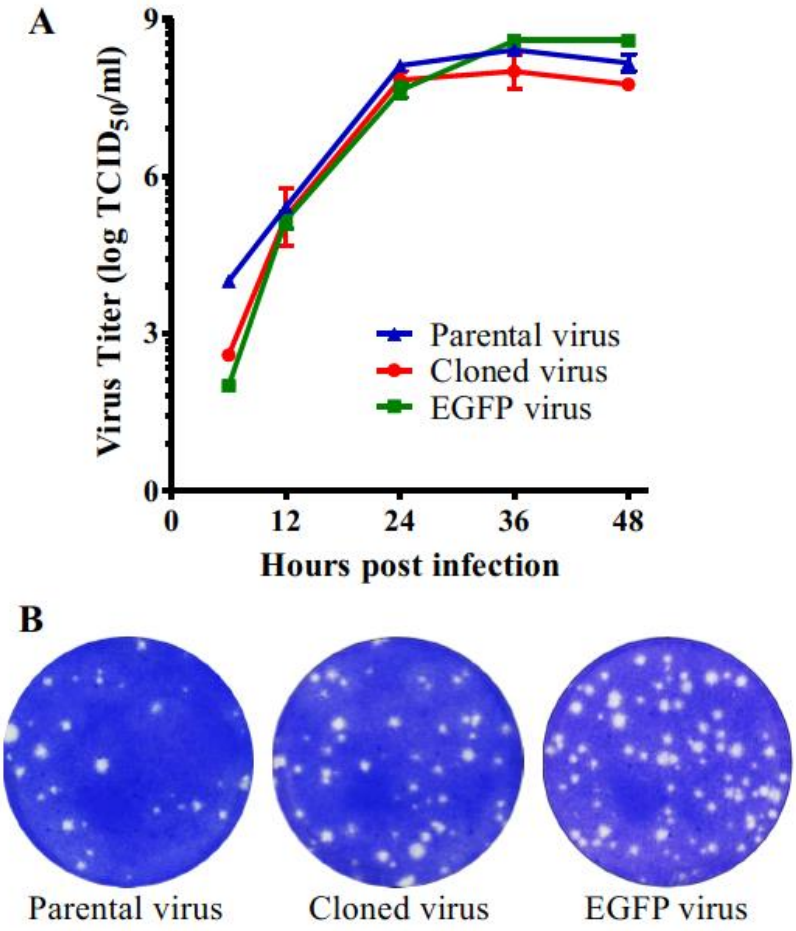

Figure 2-5. Clinical signs and surface lesions observed on infected pigs.

(**A**) Comparison of rectal temperatures among different groups of pigs. Fever is defined as temperature above 104 ºF. (**B**) Comparison of clinical scores among different groups of pigs. Clinical score of each pig was generated by scoring clinical observations of pig attitude, respiratory signs, abdominal appearance, snout lesion, oral mucosa lesion, and coronary band lesion. Each data point shown in (**A**) and (**B**) represents the mean value ± SEM from each pig group. (**C-D**). Surface lesions observed on pigs infected with the parental virus. (**C**) Vesicular lesion observed on the dorsal snout at 9 dpi. (**D**) Coronary band lesion on the left front lateral claw at 9 dpi; (**E**) Healing scar from the vesicular ulcer observed on the dorsal snout at 14 dpi. (**F**) Erosive lesion of the left front lateral claw observed during necropsy (14 dpi).

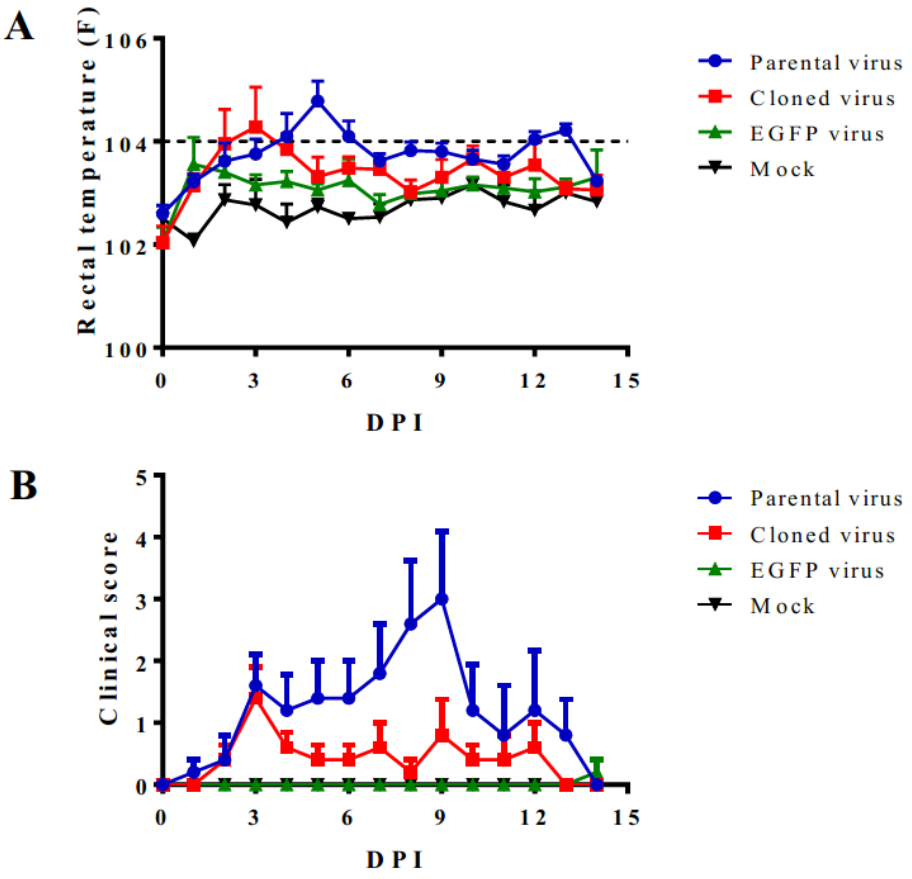


Dorsal snout lesion
Coronary band lesion
C
D
E
F
28

Figure 2-6. Comparison of viral load in pigs inoculated with the parental and recombinant viruses.

Serum, fecal swab, and nasal swab samples were collected from each individual pig at the indicated dpi, and pen (group)-based oral fluid samples were also collected at the indicated dpi. Viral loads in samples were quantified by qRT-PCR and calculated equivalent to log $TCID_{50}$/ml. (**A**) serum; (**B**) fecal swab; (**C**) nasal swab; (**D**) oral fluid. Statistical significance between different groups was indicated with asterisks (*, P<0.05; ***, P<0.001).

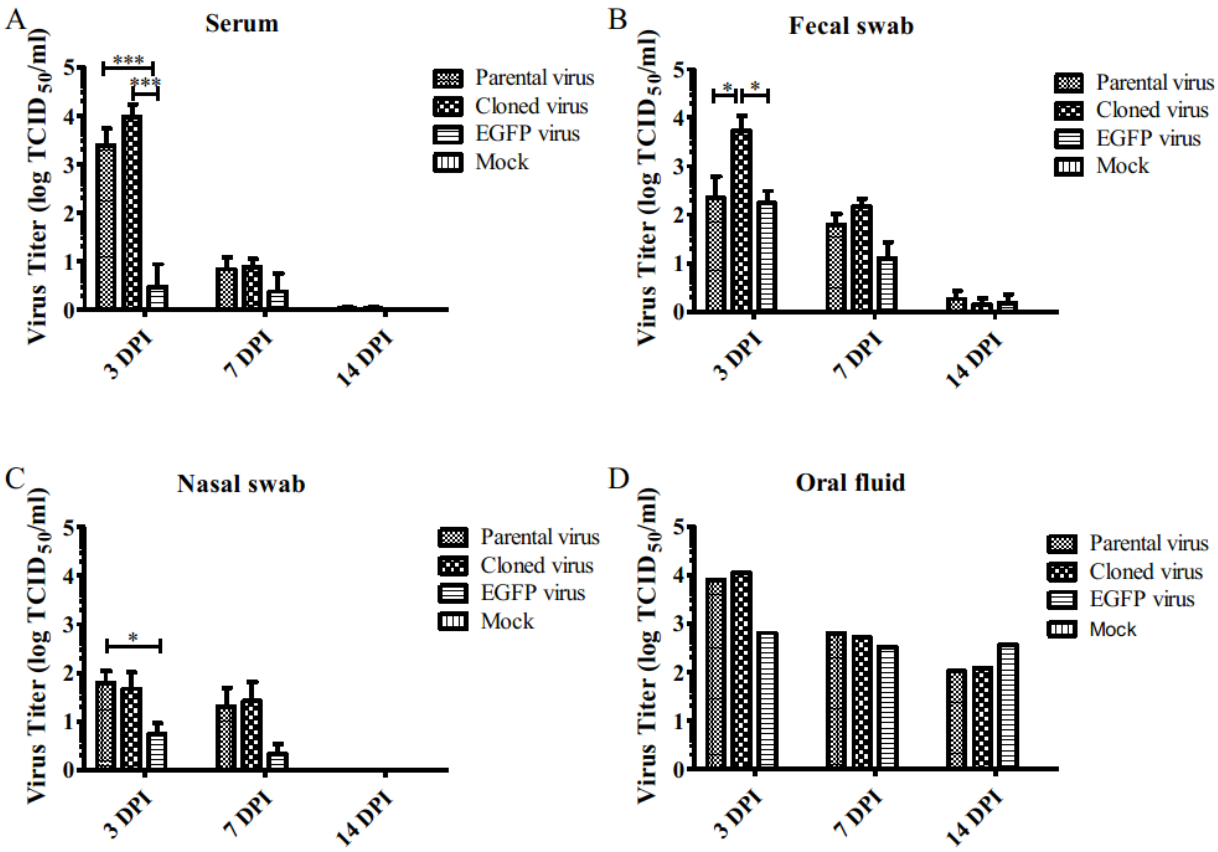

Figure 2-7. The stability of the molecular marker or reporter gene in recombinant viruses infected pigs.

(**A**) Stability of the SacI enzyme site mutation in infected pigs. Agarose gel picture showing the SacI enzyme digested DNA fragments generated by RT-PCR amplification of viral genomic region nt 3551-5227. Viral RNA was extracted from serum samples of group 1 or group 2 pigs inoculated with the SVV KS15-01 (parental virus) or vKS15-01-Clone (cloned virus) at 3 dpi, respectively. Each individual pig number is shown on top of the panel. (**B-E**) Stability of the EGFP reporter gene in pigs infected with vKS15-01-EGFP virus. Agarose gel pictures showing the DNA fragment covering the EGFP insertion region generated by RT-PCR using the RNA extracted from serum (B), oral fluid (C), fecal swab (D), and nasal swab (E) samples collected at 3 dpi. Each lane was labeled with a pig number on top of the panel. Pig #20, #30, #33, #34, #35 were from group 3 pigs that were inoculated with vKS15-01-EGFP virus; Pig #25 from mock-infected group of pigs (group 4) was included as a control. Oral fluids used in panel C were pooled samples from group 3 and group 4 pigs. (F) DNA sequencing result showing EGFP deletion in virus from serum and fecal swab samples of pig #34.

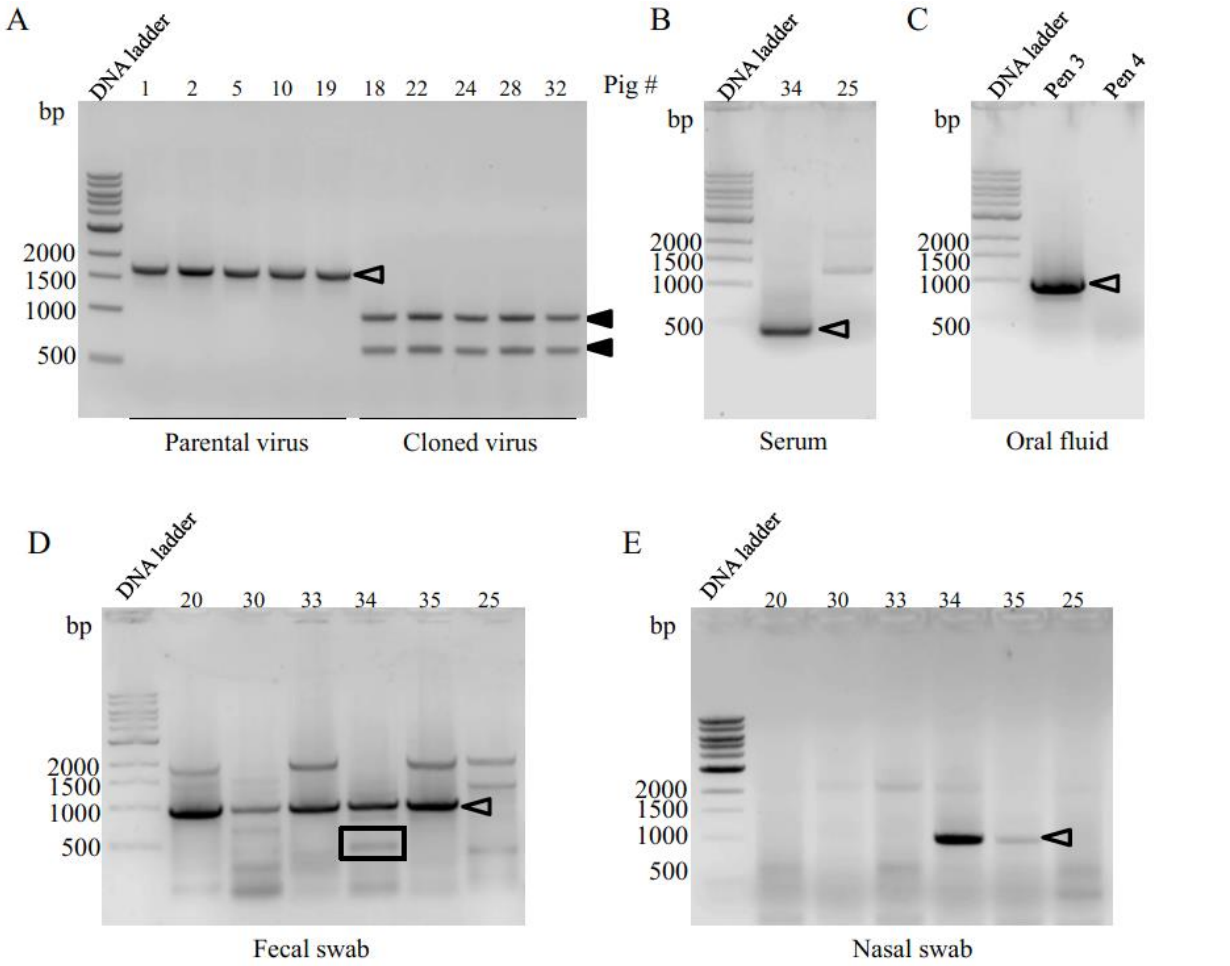
A
DNA ladder
1 2 5 10 19 18 22 24 28 32
bp
2000
1500
1000
500
Parental virus
Cloned virus
B
DNA ladder
Pig #
34 25
bp
2000
1500
1000
500
Serum
C
DNA ladder
Pen 3
Pen 4
bp
2000
1500
1000
500
Oral fluid
D
DNA ladder
20 30 33 34 35 25
bp
2000
1500
1000
500
Fecal swab
E
DNA ladder
20 30 33 34 35 25
bp
2000
1500
1000
500
Nasal swab

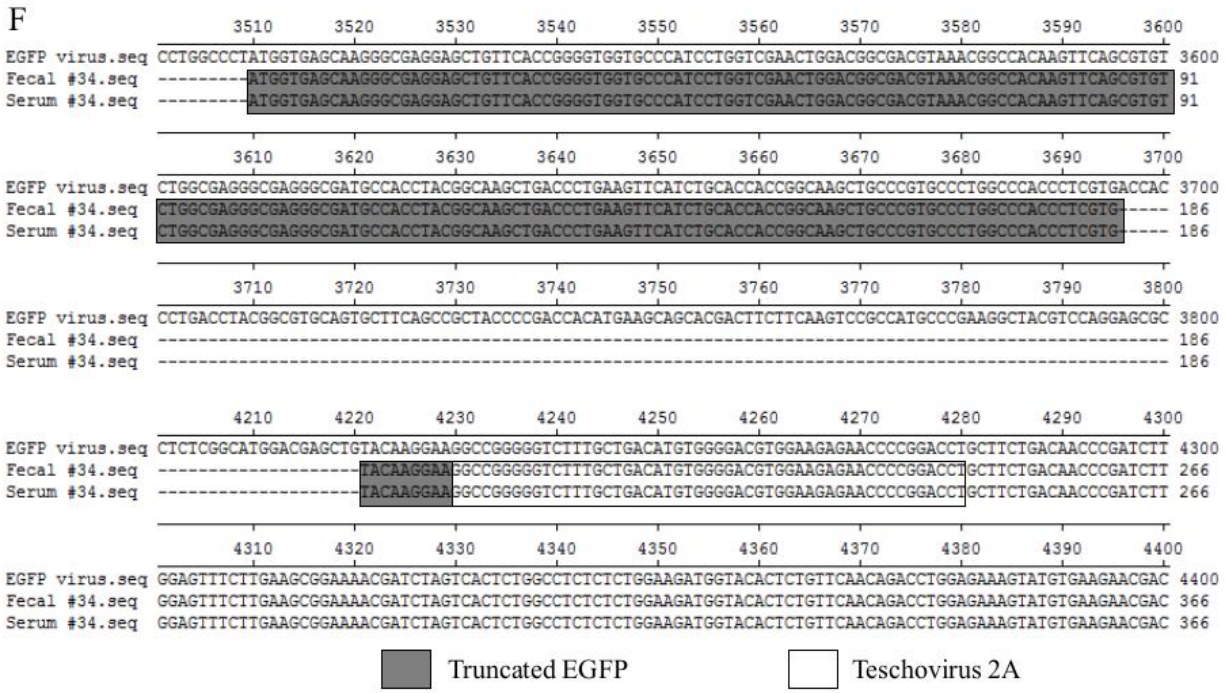
F
EGFP virus.seq
Fecal #34.seq
Serum #34.seq
Truncated EGFP
Teschovirus 2A

Figure 2-8. IFN-α response in serum samples from pigs inoculated with the parental and recombinant viruses.

IFN-α production in serum was quantified by using a ProcartaPlex Porcine IFN alpha Simplex kit (eBioscience, San Diego, CA). Samples from mock-infected pigs were included as control. Statistical analyses were performed by using one-way analysis of variance (ANOVA) followed by Tukey's *post hoc* test using GraphPad InStat Prism software (version 5.0)

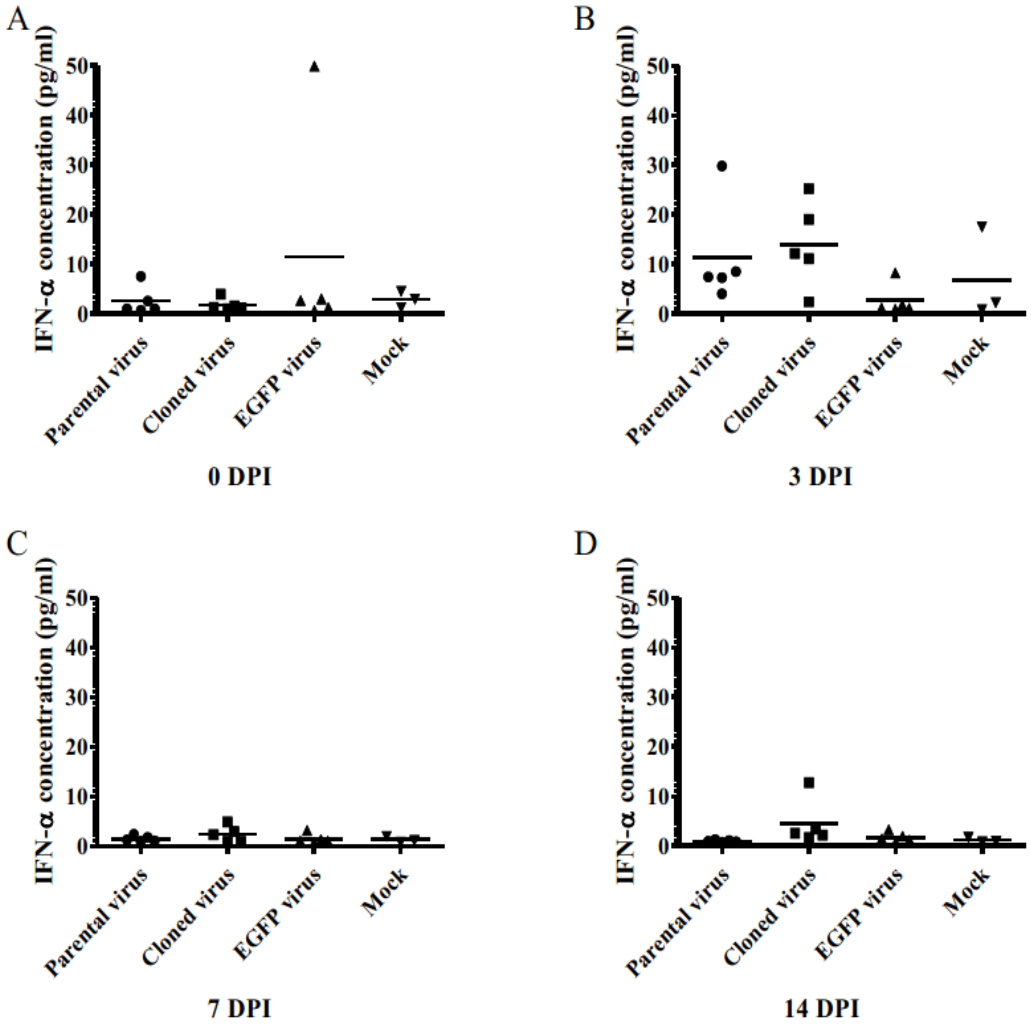

Figure 2-9. Neutralizing antibody titers in serum samples from pigs inoculated with the parental and recombinant viruses.

Neutralizing antibody assay was performed using the parental virus KS15-01; and an immunofluorescence focus assay with anti-VP2 mAb was used to determine the serum neutralizing antibody titer. The neutralizing antibody titer was defined as the highest serum dilution at which more than 90% of viral growth was inhibited. Samples from mock-infected pigs were included as control. Statistical analyses were performed by using one-way analysis of variance (ANOVA) followed by Tukey's *post hoc* test using GraphPad InStat Prism software (version 5.0)

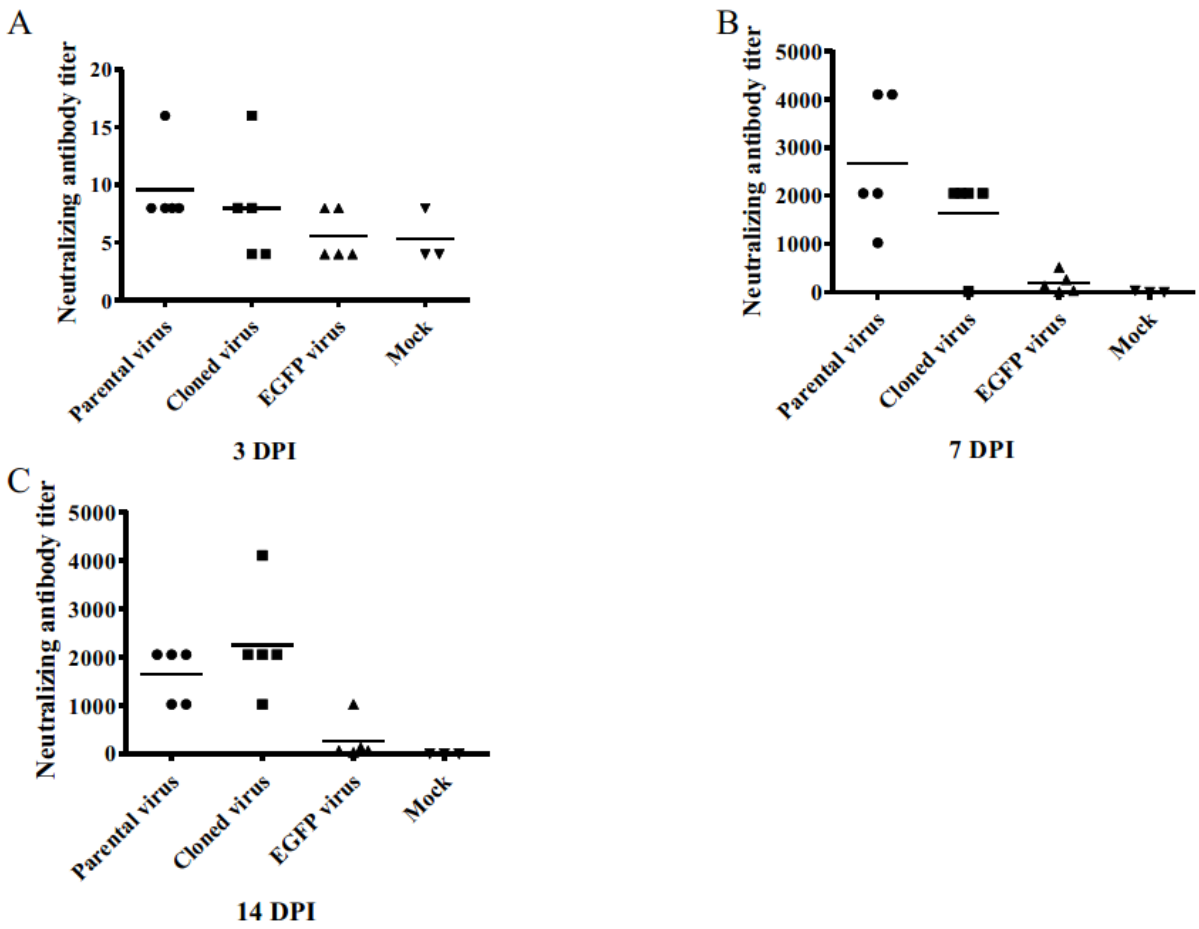

Figure 2-10. SVV specific antibody response in serum samples from pigs inoculated with parental and recombinant viruses.

Virus specific antibody (IgA, IgG, and IgM) titers were evaluated using indirect immunofluorescence assay as described in Materials and Methods. The antibody titer was defined as the highest serum dilution at which SVV proteins was detected. Serum samples from mock-infected pigs were included as control.

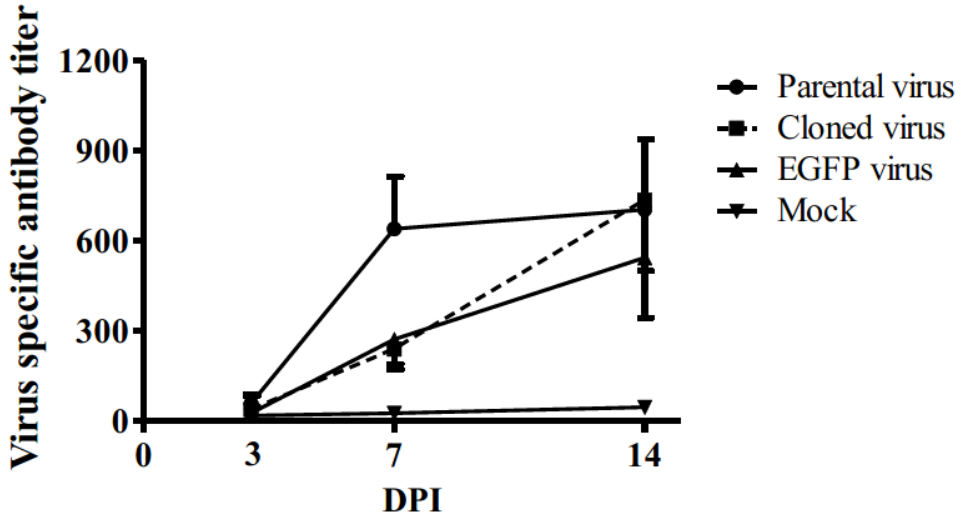

Discussion and Conclusion

In this study, we established a reverse-genetics system for an emerging SVV isolate

KS15-01. We demonstrated that the full-length cDNA clone (pKS15-01) was replication competent when transfected into BHK-21 cells; and was also infectious when passaged onto PK-15 cells. Experimental infection of pigs with the cloned virus (vKS15-01-Clone) further confirmed that the cDNA clone was infectious *in vivo*. In comparison to the parental virus, the cDNA clone contains three nucleotide mutations, including an additional U at 5' end, a G_7 to U_7 mutation at the 5' UTR, U_{7234} to C_{7234} and C_{7262} to U_{7262} mutations at the 3' UTR. These mutations may reflect the appearance of quasispecies in the virus stock or mutations introduced during the cloning process. In infected PK-15 cells, the cloned virus showed similar growth kinetics and plaque morphology to those of the parental virus. However, the pig experiment showed that the cloned virus caused slightly less clinical signs. Four pigs in group 2 showed fever and/or depression, while all pigs in group 1 showed fever and/or depression. In the group 2 pigs, no vesicular lesions were observed, but surface lesions were observed in all five of group 1 pigs. Whether the *in vivo* pathogenic differences were due to the nucleotide changes at 5' and 3' UTRs is a subject of investigation. In previous studies, the impact of the 5' UTR on the virulence of coxsackievirus B, a member of the *Enterovirus* genus in the *Picornaviridae* family, has been demonstrated (Dunn et al., 2000; M'Hadheb-Gharbi et al., 2007; Rinehart et al., 1997; Zhong et al., 2008). In addition, it was reported that the enhanced IRES activity by the 3' UTR element of FMDV determines the virulence of different isolates (Garcia-Nunez et al., 2014). As an initial analysis for the potential effect of SVV 5' and 3' UTR on the viral pathogenesis/virulence, we searched SVV full-length genome sequences that were available in the GenBank as of 03/17/2016. All three nucleotides changes observed in this study appeared in field strain sequences. An additional U at 5' end

and U_7 at the 5'-UTR are contained in the genome of SVV-001 strain and an emerged Chinese strain (CH-01-2015;(Wu et al., 2016)), while C_{7234} is observed in the genomes of three new strains in Brazil (Leme et al., 2015) and one US strain (USA/IA40380/2015; (Zhang et al., 2015)), and U_{7262} exists in the genomes of SVV-001 strain and most emerging strains. These data do not appear to provide a direct correlation between the viral pathogenesis and a specific nucleotide mutation in 5' UTR or 3' UTR region. However, to the best of our knowledge, the authentic 5' end sequence of SVV was determined for the first time in this study using 5' RACE method. For future in depth analysis, more accurate 5' UTR and 3' UTR sequences are required for field SVV strains, especially for those strains with different pathogenic/virulence properties. In addition, it is worth to note here that the cloned virus contains the nucleotide C_{4216} to T_{4216} which inactivates the SacI restriction enzyme site in 2C. Although this is a silent mutation, it is unknown whether this mutation has an effect on viral RNA structure or the expression/function of viral protein(s), which may ultimately affect the pathogenesis of the virus. Nevertheless, the SVV infectious clone generated in this study will be a useful tool allowing us to introduce site-direct mutations to 5', 3' UTR or other genomic regions to identify the key nucleotide(s) important for the pathogenesis of the virus.

One of the important applications of the infectious clone is to serve as viral backbone for the expression of foreign genes. EGFP-tagged virus is an important tool to study the basic viral biology, pathogenesis and development of marker vaccines (Fang et al., 2008; Fang et al., 2006; Fukuyama et al., 2015; Zhao et al., 2015). In a previous study (Poirier et al., 2012), a recombinant EGFP-expressing reporter virus, SVV-GFP, was constructed using prototypic

strain SVV-001. The reporter virus was used for developing a SVV-based oncolytic agent, which was only characterized in lung cancer cell lines and tumor-bearing mice, but not in the natural host cells and animals. In this study, we generated an EGFP-tagged SVV using the strain KS15-01 that isolated from infected pigs, and the recombinant virus was characterized in porcine kidney cells and nursery pigs. We adapted the foreign gene insertion site identified previously (Poirier et al., 2012), in which a EGFP gene was inserted between 2A and 2B. *In vitro* growth characterization showed that the EGFP-tagged recombinant virus vKS15-01-EGFP had similar growth kinetics and plaque morphology as those of parental virus SVV KS15-01 (Fig. 2-4). This result is consistent with the previous report that proliferation kinetics of SVV-001 and SVV–GFP were indistinguishable (Poirier et al., 2012). However, when vKS15-01-EGFP virus was inoculated into the pigs, it was only detected in serum samples from one of the five inoculated pigs (pig #34 in group 3). Sequencing result showed that viral RNA from the serum of pig #34 contains 525-bp deletion in EGFP gene, resulted the recombinant virus expressing 195-bp fragment of EGFP. The partial EGFP insertion appeared to attenuate the *in vivo* growth ability of the virus, in which the virus titer in serum was about 653-fold and 3-fold lower than that of parental virus at 3 dpi and 7 dpi, respectively. Interestingly, intact full-length EGFP was detected in nasal swab and fecal materials from all five pigs inoculated with vKS15-01-EGFP virus. The intact EGFP virus could be trapped at certain sites inside the pig, and then being expelled out from the body through nasal secretion and fecal discharge. The impaired growth ability reflected to the attenuated pathogenic properties of the virus, in which no significant clinical signs and vesicular lesions were observed in those pigs inoculated with EGFP virus. Taken together, our

data demonstrated the flexibility of the viral genomic region around 2A and 2B; however, the SVV genome may have size limitation for a foreign gene insertion. The mechanism for tolerating foreign gene insertion between 2A and 2B (or other alternative sites) of SVV genome remains to be determined. Furthermore, foreign gene insertion impaired the viral growth ability at certain level *in vivo*, resulting in attenuated pathogenic properties.

Our data from immunological analysis suggested that the humoral immunity plays an important role for SVV clearance. We analyzed innate and cell mediated immunity by measuring the expression levels of two representative IFNs, IFN-α and IFN-γ. Only minimal levels of IFN-α were detected in serum samples from pigs of group 1 (9.8 pg/ml) and group 2 (14.0 pg/ml) at 3 dpi, but the levels are not significant different from that of Mock-control group (6.9 pg/ml). IFN-γ was un-detectable in all groups of pigs through the time course of study. In contrast to the IFN response, both group 1 and 2 pigs developed rapid neutralizing antibody responses with high levels of SN titers being detected as early as 3 dpi. At 7 dpi, a significant increase in neutralizing antibodies were observed with the mean SN titers reaching 1:2779 in group 1 pigs and 1:1642 in group 2 pigs; such a high level of SN titers was remained at 14 dpi. Increased SN titers correlated well with the decreased viral titer in serum, nasal secretion and fecal material through the time course of study. The virus appeared to be cleared from the circulation and other local sites at 14 dpi. In group 3 pigs, a certain level of SN antibody was induced in four of the pigs, especially in pig #34 with SN titer of 1:256 at 7 dpi and 1:1024 at 14 dpi, suggesting that active viral replication is required to stimulate neutralizing antibody response. The level of SN Ab also correlated with viral clearance in group 3 pigs. However, an EGFP specific antibody response was not detected in serum

samples from any of the pigs in group 3 (data not shown). For the four pigs that retained the full-length EGFP gene but no detectable virus in serum, it is unknown how much viral replication occurred at local tissue sites and whether the EGFP protein was expressed to a level sufficient to stimulate an antibody response. Initially, we expected to obtain a certain level of EGFP-specific antibody from pig#34, but there was no significant difference in the antibody titers between pig#34 and other pigs in group 3 and group4. The truncated EGFP peptide (aa 1-62 and aa 237-239) produced in pig#34 may not be antigenic or the EGFP specific antibody response was lower than the detection limit. Taken together, our data suggest that the SVV 2A and 2B junction could be a potential site for introducing foreign marker genes; however, further studies are needed to manipulate the size of the foreign gene and insertion strategies to optimize the growth ability and immunogenicity of the recombinant virus.

In conclusion, we successfully developed a reverse genetic system for an emerging SVV and explored the *in vivo* growth and pathogenic properties of the parental and cloned viruses. We believe that the SVV infectious clones and the information generated from this study will have significant contributions for the future study of basic viral biology and development of control measures for SVV.

Chapter 3 – Future research on SVV

A reverse-genetics system for emerging SVV isolate KS15-01 was established in our study. *In vivo* and *in vitro* pathogenesis of this system were analyzed, and some differences were demonstrated. On the basis of what we observed on nucleotide changes at 5' and 3' UTR and the pathogenetic differences between group 1 and group 2, one aspect of future research can be investigation of the functions of 5' and 3' UTR relating to the pathogenicity of SVV. SVV strains with different virulent properties may exist in the field, and more accurate sequence of the two ends is needed. Different virulent strains affected by changes of 5' and 3' UTR were reported in other members of *Picornaviridae* family (Rinehart and Gomez et al., 1997; Zhong and Li et al., 2008; Yeh and Wang et al., 2011). Mutations of one nucleotide within 5' UTR can influence the virulence of coxsackievirus B1(Zhong and Li et al., 2008), and it was reported that a single nucleotide in the stem loop of 5' UTR leads to virulence change of enterovirus 71 in mice (Yeh and Wang et al., 2011). Therefore, utilizing our reverse-genetic system, we can further manipulate the infectious clone by point-mutation of 5' and 3' UTR to investigate its functions. In this way, different virulent strains of SVV can be distinguishable, which thus provide scientific basis for countering measures against the disease.

Infectious clone can be a powerful tool to study functions of viral genes. Compared to members of the most closing cardioviruses, 2A of SVV is significantly different in size with only 9aa. In terms of most members in *Picornaviridae*, 2A protein, on one hand, performs the function of ribosome-skipping to allow P1-2A to separate from the elongation polyprotein; on the other hand, it inhibits the cap-dependent mRNA translation, thus shut off host protein

expression. Hence, function performed by 2A protein is subject to be investigated using reverse genetics. 2A gene in SVV can be replaced with a normal, longer 2A from another picornavirus that is known to perform above two functions. And expression levels of host cell proteins after virus infection can be measured and compared to determine the function of 2A protein in SVV. Besides the scope of reverse genetics, more aspects of SVV pathogenesis need to be studied. Senecavirus is also oncolytic and has selective tropism for cancer cells featured with neuroendocrine. However, during the infection in pigs, targeted organs and tissues types are not studied yet. Using immunological methods like immunohistochemistry (IHC), viruses in tissues can be stained with anti-SVV antibodies. Figuring out distribution of SVV in host organ and tissues could help further determine transmission pathway of the disease, thus help developing counter measures to the virus.

To utilize SVV infectious clone as a viral backbone expressing foreign genes, more research work is needed to further investigate the inserted gene size fitting the backbone. Our study demonstrated that partial deletion of EGFP insertion between 2A and 2B took place *in vivo* studies and viruses seem to be attenuated, exhibiting impaired growth ability. Therefore, size of foreign gene needs to be manipulated; simultaneously, other alternative insertion sites also should be further investigated. This infectious clone has the potential to be manipulated to serve as marker vaccines for serological monitoring of vaccinated individuals and differentiation of vaccine strains with field ones in the future. Additionally, recombinant genomic RNA of viruses can be introduced into cells and further expressing viral/foreign genes. By using this property, we can insert highly immunogenic genes from another virus into the SVV infectious clone, and investigate its immune response against another virus in

vivo, thus serve as a potential chimeric vaccine.

SVV specific diagnostics is another important area that needs to be further developed. Vesicular signs, like ruptured vesicles on the snout and coronary band of hoof, can be caused by several agents such as foot-and-month disease virus (FMDV), swine vesicular disease virus (SVDV), vesicular stomatitis virus (VSV), vesicular exanthema of swine virus (VESV), and also Seneca Valley Virus (SVV). However, diagnostic assays available to differentiate one disease from another are very limited. Monoclonal antibodies that is specific to SVV can be a helpful tool for rapid diagnosis of the disease. Multiplex real-time PCR designed for these five viruses is also a very powerful method that can identify the causative agent in a rapid, effective manner. Availability of rapid diagnostics could certainly help farmers take timely measures to fight against the disease, thus minimize economic losses.

References

Adams, M.J., Lefkowitz, E.J., King, A.M., Bamford, D.H., Breitbart, M., Davison, A.J., Ghabrial, S.A., Gorbalenya, A.E., Knowles, N.J., Krell, P., Lavigne, R., Prangishvili, D., Sanfacon, H., Siddell, S.G., Simmonds, P., Carstens, E.B., 2015. Ratification vote on taxonomic proposals to the International Committee on Taxonomy of Viruses (2015). Arch Virol 160, 1837-1850.

Brown, E., Lawson, S., Welbon, C., Gnanandarajah, J., Li, J., Murtaugh, M.P., Nelson, E.A., Molina, R.M., Zimmerman, J.J., Rowland, R.R., Fang, Y., 2009. Antibody response to porcine reproductive and respiratory syndrome virus (PRRSV) nonstructural proteins and implications for diagnostic detection and differentiation of PRRSV types I and II. Clin Vaccine Immunol 16, 628-635.

Donnelly, M.L., Luke, G., Mehrotra, A., Li, X., Hughes, L.E., Gani, D., Ryan, M.D., 2001. Analysis of the aphthovirus 2A/2B polyprotein 'cleavage' mechanism indicates not a proteolytic reaction, but a novel translational effect: a putative ribosomal 'skip'. J Gen Virol 82, 1013-1025.

Dunn, J.J., Chapman, N.M., Tracy, S., Romero, J.R., 2000. Genomic determinants of cardiovirulence in coxsackievirus B3 clinical isolates: localization to the 5' nontranslated region. J Virol 74, 4787-4794.

Fang, Y., Christopher-Hennings, J., Brown, E., Liu, H., Chen, Z., Lawson, S.R., Breen, R., Clement, T., Gao, X., Bao, J., Knudsen, D., Daly, R., Nelson, E., 2008. Development of genetic markers in the non-structural protein 2 region of a US type 1 porcine reproductive and respiratory syndrome virus: implications for future recombinant marker vaccine development. J Gen Virol 89, 3086-3096.

Fang, Y., Rowland, R.R., Roof, M., Lunney, J.K., Christopher-Hennings, J., Nelson, E.A., 2006. A full-length cDNA infectious clone of North American type 1 porcine reproductive and respiratory syndrome virus: expression of green fluorescent protein in the Nsp2 region. J Virol 80, 11447-11455.

Fukuyama, S., Katsura, H., Zhao, D., Ozawa, M., Ando, T., Shoemaker, J.E., Ishikawa, I., Yamada, S., Neumann, G., Watanabe, S., Kitano, H., Kawaoka, Y., 2015. Multi-spectral

fluorescent reporter influenza viruses (Color-flu) as powerful tools for in vivo studies. Nat Commun 6, 6600.

Garcia-Nunez, S., Gismondi, M.I., Konig, G., Berinstein, A., Taboga, O., Rieder, E., Martinez-Salas, E., Carrillo, E., 2014. Enhanced IRES activity by the 3'UTR element determines the virulence of FMDV isolates. Virology 448, 303-313.

Graves, J.H., 1973. Serological relationship of swine vesicular disease virus and Coxsackie B5 virus. Nature 245, 314-315.

Hales, L.M., Knowles, N.J., Reddy, P.S., Xu, L., Hay, C., Hallenbeck, P.L., 2008. Complete genome sequence analysis of Senecavirus A-001, a novel oncolytic picornavirus. J Gen Virol 89, 1265-1275.

Hause, B.M., Myers, O., Duff, J., Hesse, R.A., 2016. Senecavirus A in United States Pigs, 2015. Emerg Infect Dis. Accepted.

Ho, S.N., Hunt, H.D., Horton, R.M., Pullen, J.K., Pease, L.R., 1989. Site-directed mutagenesis by overlap extension using the polymerase chain reaction. Gene 77, 51-59.

Inoue, T., Suzuki, T., Sekiguchi, K., 1989. The complete nucleotide sequence of swine vesicular disease virus. J Gen Virol 70 (Pt 4), 919-934.

J. Lindsay Whitton, C. T. C. a. R. F., 2005. Host and virus determinants of picornavirus pathogenesis and tropism. Nature Reviews | Microbiology, Volume 3, 765-776.

Jing-Yi Lin, T.-C. C. K.-F. W. S.-C. C. L.-L. C. a. S.-R. S., 2009. Viral and host proteins involved in picornavirus life cycle. Journal of Biomedicine Science, 16(103), 1-14.

Knowles, N., Hallenbeck, P., 2005. A new picornavirus is most closely related to cardioviruses, Abstract of the EUROPIC 2005–13th meeting of the European Study Group on the Molecular Biology of Picornaviruses; Lunteren, the Netherlands, pp. 23-29.

Knowles, N.J., Hales, L.M., Jones, B.H., Landgraf, J.G., House, J.A., Skele, K.L., Burroughs, K.D., Hallenbeck, P.L., 2006. Epidemiology of Senecavirus A: identification and characterization of isolates from pigs in the United States. Northern Lights EUROPIC.

Leme, R.A., Zotti, E., Alcantara, B.K., Oliveira, M.V., Freitas, L.A., Alfieri, A.F., Alfieri, A.A., 2015. Senecavirus A: An Emerging Vesicular Infection in Brazilian Pig Herds. Transbound Emerg Dis 62, 603-611.

Rinehart, J. E. and R. M. Gomez, et al. (1997). "Molecular determinants for virulence in

coxsackievirus B1 infection." J Virol 71 (5): 3986-91.

Lawrence, P. and J. M. Pacheco, et al. (2013). "Foot-and-mouth disease virus (FMDV) with a stable FLAG epitope in the VP1 G-H loop as a new tool for studying FMDV pathogenesis." Virology 436 (1): 150-61.

Li, Y.H., Tas, A., Snijder, E.J., Fang, Y., 2012. Identification of porcine reproductive and respiratory syndrome virus ORF1a-encoded non-structural proteins in virus-infected cells. J Gen Virol 93, 829-839.

M'Hadheb-Gharbi, M.B., Paulous, S., Aouni, M., Kean, K.M., Gharbi, J., 2007. The substitution U475 --> C with Sabin3-like mutation within the IRES attenuate Coxsackievirus B3 cardiovirulence. Mol Biotechnol 36, 52-60.

Pasma, T., Davidson, S., Shaw, S.L., 2008. Idiopathic vesicular disease in swine in Manitoba. Can Vet J 49, 84-85.

Poirier, J.T., Reddy, P.S., Idamakanti, N., Li, S.S., Stump, K.L., Burroughs, K.D., Hallenbeck, P.L., Rudin, C.M., 2012. Characterization of a full-length infectious cDNA clone and a GFP reporter derivative of the oncolytic picornavirus SVV-001. J Gen Virol 93, 2606-2613.

Reddy, P.S., Burroughs, K.D., Hales, L.M., Ganesh, S., Jones, B.H., Idamakanti, N., Hay, C., Li, S.S., Skele, K.L., Vasko, A.J., Yang, J., Watkins, D.N., Rudin, C.M., Hallenbeck, P.L., 2007. Senecavirus A, a systemically deliverable oncolytic picornavirus, and the treatment of neuroendocrine cancers. J Natl Cancer Inst 99, 1623-1633.

Reed, L.J., Muench, H., 1938. A simple method of estimating fifty per cent endpoints. American journal of epidemiology 27, 493-497.

Rinehart, J.E., Gomez, R.M., Roos, R.P., 1997. Molecular determinants for virulence in coxsackievirus B1 infection. J Virol 71, 3986-3991.

Rowland, R.R.R., Chauhan, V., Fang, Y., Pekosz, A., Kerrigan, M., Burton, M.D., 2005. Intracellular localization of the severe acute respiratory syndrome coronavirus nucleocapsid protein: Absence of nucleolar accumulation during infection and after expression as a recombinant protein in Vero cells. J Virol 79, 11507-11512.

Rueckert, R.R., Wimmer, E., 1984. Systematic nomenclature of picornavirus proteins. J Virol 50, 957-959.

Singh, K., Corner, S., Clark, S., Scherba, G., Fredrickson, R., 2012. Senecavirus A and

vesicular lesions in a pig with idiopathic vesicular disease. Journal of Veterinary Science & Technology 2012.

Sangita Venkataraman, S. P. R. J. L. N. I. P. L. H. a. V. S. R., 2008. Structure of Seneca Valley Virus-001, An oncolytic picornavirus representing a new genus. Structure, 16(10), 1555-1561.

Vannucci, F.A., Linhares, D.C., Barcellos, D.E., Lam, H.C., Collins, J., Marthaler, D., 2015. Identification and Complete Genome of Senecavirus A in Vesicular Fluid and Sera of Pigs Affected with Idiopathic Vesicular Disease, Brazil. Transbound Emerg Dis 62, 589-593.

Willcocks, M.M., Locker, N., Gomwalk, Z., Royall, E., Bakhshesh, M., Belsham, G.J., Idamakanti, N., Burroughs, K.D., Reddy, P.S., Hallenbeck, P.L., Roberts, L.O., 2011. Structural features of the Senecavirus A internal ribosome entry site (IRES) element: a picornavirus with a pestivirus-like IRES. J Virol 85, 4452-4461.

Wu, Q., Zhao, X., Chen, Y., He, X., Zhang, G., Ma, J., 2016. Complete Genome Sequence of Senecavirus A CH-01-2015 Identified in China. Genome Announc 4.

Yang, M., van Bruggen, R., Xu, W., 2012. Generation and diagnostic application of monoclonal antibodies against Senecavirus A. J Vet Diagn Invest 24, 42-50.

Yeh, M. T. and S. W. Wang, et al. (2011). "A single nucleotide in stem loop II of 5'-untranslated region contributes to virulence of enterovirus 71 in mice." PLoS One 6 (11): e27082.

Zhong, Z. and X. Li, et al. (2008). "Mutations at nucleotides 573 and 579 within 5'-untranslated region augment the virulence of coxsackievirus B1." Virus Res 135 (2): 255-9.

Zhang, J., Pineyro, P., Chen, Q., Zheng, Y., Li, G., Rademacher, C., Derscheid, R., Guo, B., Yoon, K.J., Madson, D., Gauger, P., Schwartz, K., Harmon, K., Linhares, D., Main, R., 2015. Full-Length Genome Sequences of Senecavirus A from Recent Idiopathic Vesicular Disease Outbreaks in U.S. Swine. Genome Announc 3.

Zhao, D., Fukuyama, S., Yamada, S., Lopes, T.J., Maemura, T., Katsura, H., Ozawa, M., Watanabe, S., Neumann, G., Kawaoka, Y., 2015. Molecular Determinants of Virulence and Stability of a Reporter-Expressing H5N1 Influenza A Virus. J Virol 89, 11337-11346.

Zhong, Z., Li, X., Zhao, W., Tong, L., Liu, J., Wu, S., Lin, L., Zhang, Z., Tian, Y., Zhang, F., 2008. Mutations at nucleotides 573 and 579 within 5'-untranslated region augment the

virulence of coxsackievirus B1. Virus Res 135, 255-259.

Publisher's Permission for Reproducing Published Materials

Chapter 2 related:

http://www.sciencedirect.com/science/article/pii/S0042682216301702

Virology - Journal author rights

Personal use

Authors can use their articles, in full or in part, for a wide range of scholarly, non-commercial purposes as outlined below:

- Use by an author in the author's classroom teaching (including distribution of copies, paper or electronic)
- Distribution of copies (including through e-mail) to known research colleagues for their personal use (but not for Commercial Use)
- **Inclusion in a thesis or dissertation** (provided that this is not to be published commercially)
- Use in a subsequent compilation of the author's works
- Extending the Article to book-length form
- Preparation of other derivative works (but not for Commercial Use)
- Otherwise using or re-using portions or excerpts in other works

These rights apply for all **Elsevier authors** who publish their article as either a subscription article or an open access article. In all cases we require that all Elsevier authors always include a full acknowledgement and, if appropriate, a link to the final published version hosted on Science Direct.